UNIVERSITÀ DEGLI STUDI DI PADOVA

Dipartimento di Fisica e Astronomia "Galileo Galilei"

Corso di Laurea Magistrale in Fisica

Tesi di Laurea

In-cell recordings with 3D microelectrode arrays

Relatore

Prof.Flavio Seno

Correlatore

Dr. Ghunter Zeck

Laureando

Luca Del Torre

Anno Accademico 2017/2018

Abstract

Micro Electrode Arrays (MEAs) have been used for 40 years to record extracellular signal from electrically excitable cells. The development of three dimensional microstructured electrodes has been shown to improve the electrical contact between cell and electrode. This can allow to reduce the electrode dimensions to improve spatial resolution, to have a one-to-one correspondence between cell and electrode and, applying an electrical stimulus, to obtain in-cell like recordings. In-cell like recordings resemble in their time course the transmembrane voltage obtained by an intracellular sharp electrode during electrical activity. Appropriate electrical stimulation transiently increases the leakage membrane conductance and gives access to a signal substantially different from the extracellular one.

The aim of this thesis is to develop different electrodes designs and to investigate on cardiomyocytes cell cultures the feasability of in-cell recordings. Standard MEAs (tip-shaped and planar electrodes) were compared with self-developed MEAs. The duration of the in-cell signal, his amplitude, the voltage threshold to induce it and his repeatability over minutes and hours were studied by varying the stimulus duration and the stimulus voltage.

We successfully processed solid and hollow pillars electrodes as well as mushroom-shaped electrodes. On these electrodes we recorded extracellular action potential from cardiomyocytes. The stimulation protocols successfully evoked in-cell like signals on all the electrodes. In-cell recordings could be obtained onto the same cell over several hours and occasionally days. Hollow pillars induced longer in-cell recording, tip-shaped electrode had a lower threshold. However the large variability of in-cell like recordings on the different electrode shapes does not suggest one particular shape to be used in future. A promising spontaneous in-cell recording was obtained in one culture, opening to future development on three-dimensional microelectrodes research.

Sommario

I Micro Electrode Array (matrici di micro elettrodi) sono stati usati negli ultimi 40 anni per registrare segnale extracellulare da cellule eccitabili come i neuroni. Lo sviluppo di elettrodi tridimensionali microstrutturati ha permesso di aumentare il contatto elettrico tra cellula ed elettrodo. Questo può essere sfruttato per aumentare la risoluzione spaziale, avere una corrispondenza uno-a-uno tra cellula ed elettrodo e, applicando uno stimolo elettrico, per ottenere un segnale simil-intracellulare detto "in-cell". Questo tipo di segnale assomiglia al potenziale di membrana misurato da un elettrodo appuntito intracellulare durante un potenziale d'azione. La stimolazione elettrica infatti, aumentando transitoriamente la conducibilità della membrana da accesso ad un segnale sostanzialmente differente da quello extracellulare.

Lo scopo di questa tesi è di sviluppare diverse forme e design di elettrodo e di investigare su colture cellulari di cardiomiociti la fattibilità di registrazioni "in-cell". Oltre agli elettrodi autoprodotti, sono stati confrontati elettrodi "a punta" e planari, disponibili in commercio. Gli elettrodi sono stati confrontati cambiando la durata e la tensione dello stimolo elettrico, per valutare le variazioni nella durata del segnale "in-cell", la sua ampiezza, la soglia di tensione che lo induce, e la ripetibilità per minuti ed ore.

Abbiamo creato con successo elettrodi con la forma di cilindri pieni e vuoti e "a fungo", registrato potenziali d'azione extracellulari da cardiomiociti con essi, e ottenuto la registrazione di segnali "in-cell" con l'applicazione di protocolli di stimolazione elettrica. È stato possibile ripetere questi protocolli sulle stesse cellule per diverse ore e a volte giorni. I cilindri vuoti hanno indotto le registrazioni "in-cell" più lunghe, elettrodi a punta hanno mostrato una soglia di tensione inferiore. Ciononostante, la grande variabilità di questi risultati non suggerisce nessun tipo di forma preferenziale da usare in futuro. Un promettente segnale "in-cell" spontaneo (senza bisogno di stimolazione elettrica) è stato ottenuto in un caso, aprendo a futuri sviluppi nella ricerca sui microelettrodi tridimensionali.

Contents

Chapter 1

Introduction

1.1 Motivation

Micro electrodes array (MEA) technology was born as a non-invasive alternative to patch-clamp to record action potential of excitable cells: an array of planar electrodes being close enough to the cells, can measure variations of the potential in the cleft between the electrode and the cells; this type of measurement is called extracellular recording, because of the substantially difference with patch-clamp that measure the voltage directly inside the cells.

Extracellular recordings are not conclusive, in the way that one is not able to tell with exactly which cell one records from. Furthermore, no small modulations of the action potentials can be revealed. On the other hand, patch-clamp recording gives access but it irreversibly damages the cell. Therefore MEAs allow longer term recording for multiple cells at the same time, without needing particular skills on the experimenter. This makes possible investigation of network connectivity and communication in neuronal populations.

In recent years, there have been different approach aiming to improve the electrical coupling between electrodes and cells on MEAs using different three dimensional structures. This to increase spatial resolution without losing signal quality or to access information on small modulation of the voltage. In several works, results were obtained combining these structures with electrical stimulation, providing access to intracellular-like signals (improved amplitude and signal shape). These in-cell recordings are believed to be induced by electroporation, a well studied phenomenon usually used to load molecules and genes into the cells. It remains unclear if there is a dependence between the amplitude, duration, and simplicity in obtaining these recordings, and the shape and features of the electrodes.

Optimizing electroporation could allow a stable and repeatable multi-site access to intracellular recording, permitting the study of drugs effects in cardiomyocytes that actually can be observed only with patch-clamp. Neuronal applications could lead to the measurement of low signals as sub-threshold depolarization.

1.2 Aim and outline

The focus of my thesis is the development, characterization and testing of three dimensional microstructures on MicroElectrode arrays (MEA). During my thesis I am going to develop different electrodes shapes (mushroom-shaped, pillars, hollow pillars) of different dimensions ($2.7 - 3.7\mu m$) and designs (figure 1.1) to test them on cardiomyocytes cell culture, using electroporation protocols. The confrontation criteria will be the signal-to-noise-ratio, the voltage threshold inducing electroporation, the mean duration of the in-cell recording, the repeatability of the protocol.

The work was carried out with the following outline:

- A state of the art analysis of extracellular recordings, MEA technology and three-dimensional electrodes in chapter 2;

Row	Diameter	Number of pillars
1		1
2	2.5 μm	3
3		25
4		1
5	3.5 μm	3
6		11
7	10 μm	*planar*
8	30 μm	*planar*

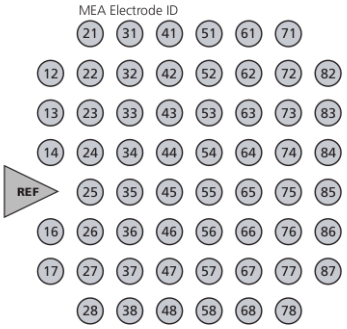

Figure 1.1 – MEA design

- Fabrication of microstructures by electroplating and electropolymerization described in section 3.1.2 and 3.1.3;
- Characterization of the different electrodes by impedance measurements and scanning electron microscopy (SEM) described in section 3.2;
- Cultivation of cardiomyocytes described in section 3.4.1;
- Development of an efficient and repeatable electroporation protocol described in section 4.1.2;
- Experiments on many cells (at least 20, up to 70) for every kind of electrode, described in section 4.1.3;
- Data analysis, focused on the confrontation between different electrodes shapes described in section 4.2;
- Discussion of the results and future developments in section 5.1.

Chapter 2

Fundamentals and state of the art

2.1 Non invasive, multi-site, simultaneous recordings on electrically excitable cells

2.1.1 Electrogenic cells: a general picture

Electrogenic cells are a class of cells, electrically active because of their capacity to regulate ions flow across the membrane. Neurons, muscle cells and some endocrine cells belongs to this category, in general they share the ability to produce an action potential. Though, to better understand the technologies used in this thesis, neurons are introduced in the following.

The neuron is the basic unit of the nervous system. It is an electrically excitable cell, whose main functions are transfer, storage and computing information. Anatomically it is schematically composed of a cell body with processes:

- dendrites, micrometer sized, functioning as receptive structures;
- the axon, usually one for each cell, that can vary between tenth of micrometers up to meters in length, providing output and input, from and to other neurons.

The structures that enable informations transfer between neurons are the synapses, axons terminals. Information transfer is performed electrically or chemically by the transfer of neurotransmitters.

The basic mechanism of information processing is caused to the action potential (AP). The cell can change the voltage over the cell membrane using ion channels and pumps:

- ion pumps keep a concentration gradient and a resting potential (about -80mV) between the inside and the outside of the cell, it is an active equilibrium;
- ion channels opening and closing are voltage or chemical dependent. When the action potential is triggered (reaching a potential threshold about -60mV), sodium channels are opening and provoking a fast depolarization (reaching +20mV), potassium channels are then opening and bringing back the potential to the resting state.

This all happens in a time course of about 1-100 ms, while currents of mA/cm^2 pass over the membrane. Action potential can flow along the axon for long distances (up to meters) and with high speeds (about 20m/s). Indeed, once an action potential is initiated at one site on an extensive membrane, it triggers action potentials at adjacent sites, thus leading to a sequence of action potentials throughout the remaining membrane.

This is the basic mechanism that allows the information transfer but the computational and storage mechanisms are due to the network behavior of neuronal systems. Indeed, the single neuron is not the location of one information or particular cognitive function, this relies to the topological and physiological structure of how neurons are connected. Each of them can receive up to thousands of input by the dendrites, coming from different neurons, and every synapse that connect neurons has different chemical and biological behavior. The complexity of this system permit the computing of all the tasks that the nervous system can perform.

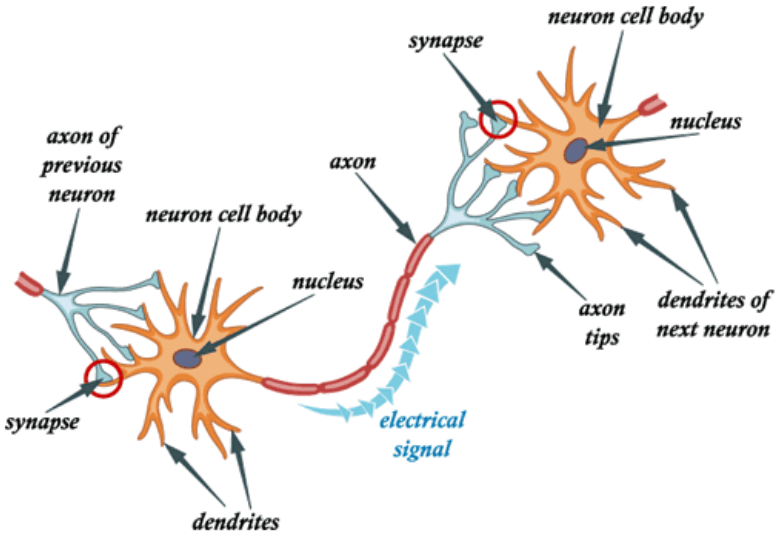

Figure 2.1 – Neuron schematic picture

This simplified picture, far to be exhaustive, gives a general idea about features that should have an experimental tool which aims to shed a light on neuronal systems. In particular, if we want to obtain informations about single cells electrical activities and their connection with the information processing we need to establish an electrical link with multiple cells simultaneously.

Direct electrical informations can be investigate penetrating into the cell, a technique called patch-clamp [18], with the drawback of damaging the cell (relative short recording time allowed) a high ability required by the experimenter and the impossibility to record simultaneously many cells. Otherwise electrical activity can be monitor from outside the cells recording electrical signal approaching the external membrane, measuring and modifying the potential between the cell and the electrode, it is called "extracellular recording".

2.1.2 Extracellular recordings

The action potential is caused by ions flowing in and out the cell. These ions come and go to the electrolyte that surrounds the cells. Therefore an electrode close enough to the cell can measure the current flow or the potential changes due to the action potential. The waveform of the extracellular signal is quite different from the intracellular action potential, but in many cases the task is to detect whether or not an action potential has occurred at a specific time.

Let's consider a cell lying over a recording electrode, and a reference electrode far from the cell but in the same electrolyte medium. It is possible to build a simplified model (point-contact model [7]) to better understand extracellular recordings. The equivalent circuit is shown in figure 2.2. In this model the membrane is divided in a junction membrane A_{JM} and a free membrane A_{FM}. The conductances for every ion species (g^i_{JM} and g^i_{FM}) and the conductance not voltage dependent (g_{Leak}), the capacitance of the membrane (c_{JM} and c_{FM}), the electrode capacitance and resistance (c_{el} and r_{el}) and the resistance of the cleft (r_{seal}) are expressed per unit area assuming homogeneity of the membrane. The electrode voltage is V_{el}, the intracellular voltage is V_M while the extracellular voltage that is measured is V_J.

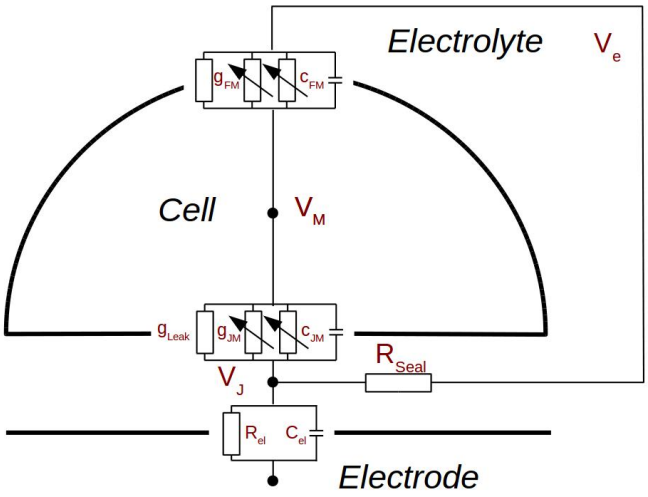

Figure 2.2 – Point-contact model of a cell over one electrode

Kirchoff's law applied to the node on the junction between the electrode and the cell:

$$\frac{(V_E - V_J)}{r_{Seal}} + \left(c_{el}(\frac{dV_{el}}{dt} - \frac{dV_J}{dt}) + \frac{V_{el} - V_j}{r_{el}} \right) + c_{JM}(\frac{dV_M}{dt} - \frac{dV_J}{dt}) + \sum_i g(v)^i_{JM} \cdot (V_M - V_J - V^i_{eq}) + g_{Leak}(V_M - V_J) = 0 \quad (2.1)$$

V_{eq} is the Nernst potential of every ion species, the equilibrium potential between electrical and diffusive forces [19]. The conductance of the ions channels is changing according to Hodgkin and Huxley model [13].

This equation can be simplified assuming:

- $V_E = 0$, the reference potential is set to ground
- A capacitive electrode (big r_{el}) with a small capacitive current response $g_J V_J > c_{el}(\frac{dV_{el}}{dt} - \frac{dV_J}{dt})$
- The voltage in the junction is small $V_M - V_J \simeq V_M$.

The equation simplified, integrated over the attached membrane:

$$V_J = R_{seal} \cdot \left(C_{JM} \frac{dV_M}{dt} + \sum_i G(v)^i_{JM} \cdot (V_M - V^i_{eq}) + G_{Leak} V_M \right) \quad (2.2)$$

This is a really simplified model but it shows why we don't expect a linear relation between intracellular and extracellular recordings, and shed a light on the role of the junction between cell and electrode: if the cell is closely attached to the electrode, R_{Seal} is big, and the measured signal V_J is large. Moreover, in most of the experimental setup, the ionic current in the junction is small, and the conductance of the junction is big enough to neglect the second and the third term in equation 2.2. In this situation the signal is purely capacitive, depending on the derivative of the intracellular waveform. We should also consider that the cells are not sitting entirely on the electrodes, therefore, the recorded signal amplitude will be proportional to the attached surface [7].

2.1.3 In-cell like recordings

One interesting but not commonly known feature of extracellular electrodes, is the opportunity to obtain in particular conditions recordings resembling intracellular ones [14, 9, 11, 36, 2, 15, 4].

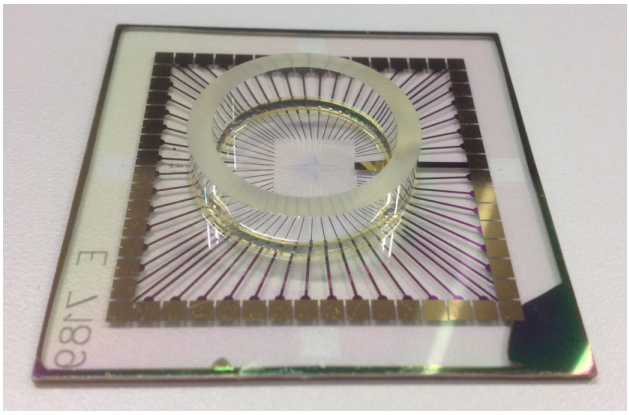

Figure 2.3 – Microelectrode Array (MEA). Comprising 60 electrodes (typical diameter: $30\mu m$)

An early report by Jenkner and Formherz [14], recording with a field-effect transistor from a neuron and injecting a current into it with a patch-clamp micro-electrode to elicit an action potential found bistability in the membrane conductance: lowering the patch electrode it was possible to switch between an "A-type coupling" to a "B-type coupling", indistinguishable in the shape from the patch-clamp recording.

There are different theories for the explanations of these phenomena, that can be induced in different ways, but ending up with a common consequence: the conductance of the membrane is critically increased, enhancing the right part of equation 2.2, leading to obtain a linear relation with the intracellular signal V_M. Therefore it is suitable to use a common term for these recordings, even if they are induced in different ways: in the following we refer to them as "in-cell recordings"

The increase of the membrane conductance has been hypothetically attributed to: self gating of ion channels [7], mechanical deformation of the membrane inducing opening of ion channels [7, 4], membrane mechanical deformation forming non-specific pores (non-ion selective channels) [4, 9], cytoskeleton restructuring recruiting voltage independent ion channels [9] and membrane nano-pores induced by electroporation [11, 36, 2, 15]. The mechanism of electroporation is explained below.

2.1.4 Micro Electrode Array (MEA)

Extracellular measurements, explained in section 2.1.2, are also performed with MicroElectrode arrays (MEA), a "non-destructive method for maintaining electrical contact with an individual culture, at a large number of points, over periods of days or weeks" [32].

MEAs consist of a carrier substrate, usually glass, on which metallic tracks and electrodes are micropatterned and insulated with photolithographic procedures. For MEA designed for in vitro experiments a glass well on top defines a culture dish in which excitable cells or tissue may be cultured. The insulating top layer, through which only the electrodes and contact pads are opened, often consists of a glassy silicon nitride layer (Si_3N_4) which is a favorable substrate for protein coating (poly-lysine, laminin, fibronectin) to improve cell adhesion. The electrodes are fabricated from different metal-based materials suitable for two-way communication – recording from and stimulation of excitable cells and tissue.

MEAs have been extensively used for about 40 years in many different experiments and studies. *In-vitro* culture, *in-vivo* and *ex-vivo* experiments; using the ability to record and stimulate from the same electrodes.

They are at the basis of our knowledge about retina functions [30, 39] and on the development of retina prosthetics. They are used to study brain slices and better understand central nervous system diseases [20]. They are adapted to study drug effects on cardiac cells [17, 5].

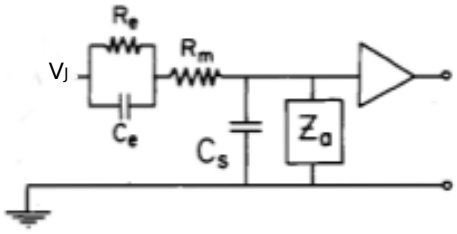

(a) Equivalent circuit for a metal electrode connected with an amplifier [23]

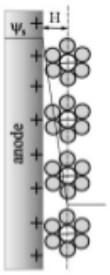

(b) Helmholtz Model, double layer capacitance [35]

Figure 2.4

2.2 Electrical properties of metal electrodes

To understand MEA functioning it is important to have an idea on how the junction voltage V_J (see sec 2.1.2) is measured. The metal electrodes (with capacitance C_e and resistance R_e) are connected with an amplifier, with a very high input impedance Z_a to not alter the signal, the conductive lane have a negligible resistance R_m and a shunt capacitance C_s that is attenuating the signal [23]. The electrical equivalent circuit considered is shown in figure 2.4a. Neglecting R_m and C_s, the voltage measured V_a is:

$$V_a = V_J \cdot \frac{Z_a}{Z_e + Z_a} \tag{2.3}$$

With Z_e impedance of the electrode. This shows already that to optimize the circuit, Z_e should be minimized.

The impedances are in general depending from the frequency. It is commonly accepted that the mean frequency of interest is 1kHz.

When the electrode is in the capacitive region ($R_e >> \frac{1}{\omega C_e}$) and Z_a is mostly a resistive term, the circuit is working as an high pass filter with cutting frequency of $\frac{1}{C_e R_a}$.

The basic model of the capacitance of a metal electrodes immersed in an electrolyte is the Helmholtz Model. Helmholtz idea was that when there is a potential difference between an electrode and an electrolyte in contact, ions and counter-ions are adsorbed to the electrode surface, and the situation is analogous to that of conventional capacitors with two planar electrodes separated by a distance H that can be approximated with the radius of the solvated ions (figure 2.4b). The planar approximation is valid for spherical shapes when the electrode radius is large enough (more than 40nm) [35], for microelectrode subject of this thesis this approximation is used.

2.3 Three dimensional microstructures

Even though the impedance of an electrode is an important influencing parameter for the signal, on a practical side, once the biological material is involved, the cell-electrode interaction become critical. Therefore, as shown in section 2.1.2, the voltage measured is directly proportional to the resistance of the cleft R_{seal} (equation 2.2) and the latter is strongly dependent on the thickness of the cleft.

Improving the cell-electrode electrical coupling has been subject of many studies, to obtain informations on weak signals, like sub-threshold synaptic potentials and ion channels property or to reduce electrode dimensions to improve spatial resolution. This can be achieved with chemical treatment that improve cell adhesion, selecting electrode's material, or modifying the shape of the electrode, with nano and micro three dimensional structures.

Nanopillars have been used to obtain spontaneous cell-membrane poration induced by the extreme sharpness and small size of the tip (coated with a phospholipid bilayer) that can disrupt the

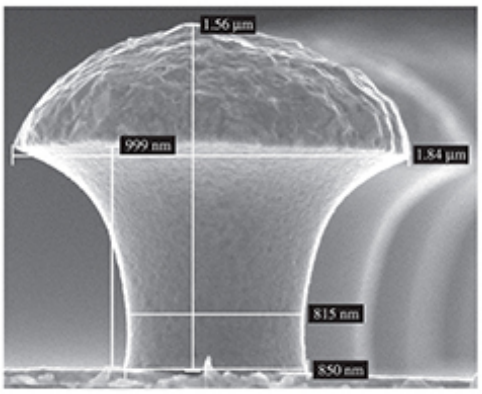

Figure 2.5 – SEM picture of a gold mushroom-shaped microelectrodes from M.Spira [28]

cell membrane [6].

In 2007 Spira *et al.* proposed a gold mushroom-shaped microelectrodes [28] ($gM\mu Es$), which shape and dimension were selected to mimic the geometry and dimensions of dendritic spines (figure 2.5). The $gM\mu Es$ were chemically functionalized to activate endocytotic-like mechanisms, aiming to "lure" the neurons to engulf the protruding electrodes. The development of these structures culminated in 2010 with spontaneous in-cell like recordings from *Aplysia* neurons and the first synaptic potentials recording with MEA [9, 10]. The engulfment of the microelectrodes is generated by molecular cascades that include the restructuring of the cytoskeleton to form an actin ring around the stalk of the 'gold mushroom' [27].

However the development of $gM\mu Es$ reproducing the same results on other neurons or cardiomyocytes has proved to be harder, so far only study on feasibility on mammalian neurons [21] and loose-patch-like junctions on hippocampal neurons [26] has been published (for a complete review of Spira's work see [29]).

2.4 Electroporation

An alternative way to use 3D structures to obtain in-cell recordings for a short time is to apply bursts of electrical pulses and record from the same electrode that applied the stimulus. The in-cell like signal is commonly attributed to electroporation: the transmembrane electric field induced by the stimulation opens nano-holes on the cell membrane, close to the stimulation electrode, this enhance the ion conductance of the membrane, G_{Leak} in equation 2.2 (the holes are non-selective), increasing the relevance of the linear term of V_m on equation 2.1.

From the early studies of cell membrane conductivity it is known that an intense transmembrane electric field can increase dramatically the ions conductivity. However, this has been studied mostly to understand cells ions leakage when applying electric shocks and to load molecules and genes into the cell using the permeability induced by the holes opening [34].

In early years many studies on cardiomyocytes has been published using micro [11, 2] and nano [36, 15] electrodes, with electroporation protocols. This technique allowed a multisite simultaneous access to in-cell recordings repeatable over a period of days, since it is not harmful for the cells. It has proved to be effective on studying membrane repair dynamics [11] and drugs screening [2].

Chapter 3

Three dimensional MEAs and cell culture

3.1 Microelectrode array fabrication

The MEA fabrication process is schematically illustrated in figure 3.1.

The basis for the MEA is a square glass wafer of side length 49 mm. Gold is sputtered on these, which is structured into feedlines by means of a lift-off process. Subsequently, a plasma enhanced chemical vapor deposition (PECVD) is performed and one layer Silicon nitride (SiN_x) is applied as an insulator. The insulator is then covered with photoresist (AZ ECI 3027) by means of spin coating (figure 3.1).

After partial UV exposure of the substrate through a mask, the photoresist is removed from the exposed areas with a developer. Subsequent plasma etching (CDE) removes the insulator at the exposed areas (figure 3.1 Step 4).

The three dimensional structures are now electroplated and rinsing of the substrate in potassium hydroxide remove the remaining photoresist. Finally the electrodes were coated with poly(3,4-ethylenedioxythiophene) (PEDOT) by electropolymerization.

My contribution to the production starts at the electroplating phase (figure 3.1 Step 6).

3.1.1 Cyclic voltammetry

The quality of the previous steps was qualitatively checked with cyclic voltammetry in a 0.5M sulfuric acid bath, with a three-electrode configuration (figure 3.4a).

Cyclic voltammetry is based on a ramp between two potentials covered on both ways with a certain scan rate. This triangular potential is usually repeated many times. The current as a function of potential is called a cyclic voltammogram (CV) (figure 3.2a).

Setting a potential range of the CV wide enough to induce oxidation, metal electrodes can be electrochemically "cleaned": In the oxidative part of the scan, surface contaminations and active sites on the surface get oxidized, creating functional groups. In the reductive scan these groups and all oxidized species get removed and the active sites on the electrode surface are restored. From this reduction peak it is possible to calculate the real surface area of an electrode (figure 3.2b). Comparing CV of different channels we can easily understand if one of the sites was not properly "opened" on the previous step.

The potential was scanned from 0.4 to 1.4 V with a scan rate of 0.1V/s, and the cycle was repeated 30 times.

3.1.2 Electroplating

The electrodeposition process is based on an electrochemical cell where the cathode is the part to be plated. The applied potential difference drive the ions solved in the electrolyte to the cathode surface with sufficient energy to induce a reduction reaction (figure 3.4a).

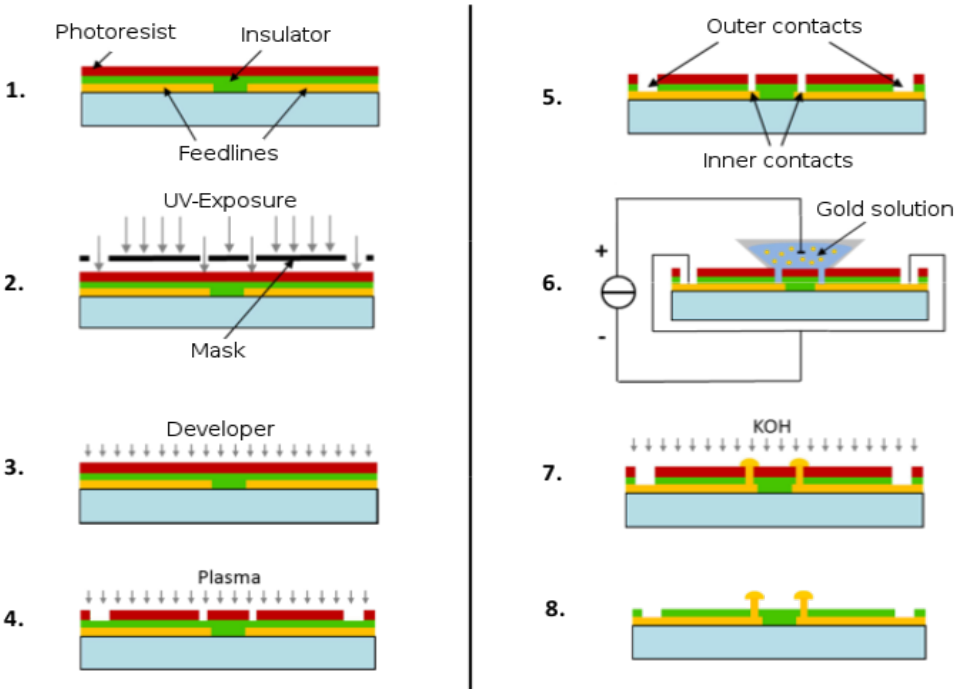

Figure 3.1 – MEA production

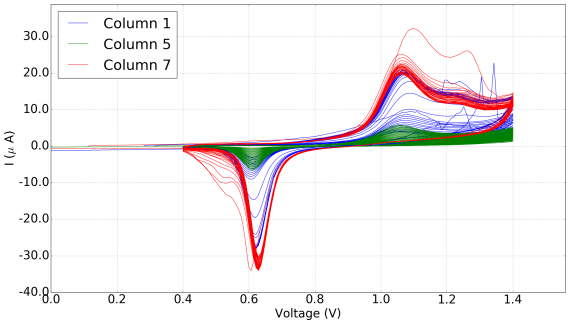

(a) I vs V: the negative peak is due to the oxygen desorbiment. Not properly opened channels results in much smaller figures (e.g. column 5). Note that along cycles the shape is changing, leading to similar shapes for column 1 and 7 (the gold surface is cleaning).

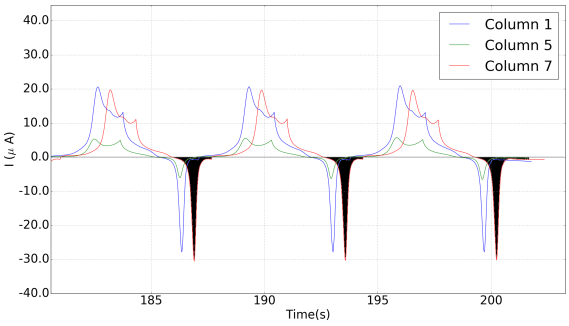

(b) I vs t: last 3 cycles: the black area, allow an estimation of the column 7 gold surface $A = \frac{Q}{390\mu C/cm^2}$ according with [33] (oxygen is chemisorbed in a monoatomic layer with a one-to-one correspondence with gold surface atoms)

Figure 3.2 – Cyclic voltammetry. 3 channels of the fourth row of a MEA (see table 1.1 for the design)

		Mushrooms		Hollow Pillars		Mushroom-shaped	
Row	Diameter μm	Volume μm^3	t_{Au}	Volume μm^3	t_{Au}	Volume μm^3	t_{Au}
1		15.9		10.8		48.6	20'39"
2	2.6	49.6	31'3"	32.5	31'31"	147.7	20'8"
3		430.4		271		1248.5	19'35"
4		31.9		14.1		121.7	25'45"
5	3.6	91.5	31'3"	43.8	31'31"	360.9	26'38"
6		331.3		159.4		1319	26'53"

Table 3.1 – Volume calculation and gold deposition time. The diameter was measured with an optical microscope for many holes (figure 3.3) and mediated. The current density used for pillars is $0.015 nA/\mu m^2$, for hollow pillars and mushrooms is $0.07 nA/\mu m^2$.

In order to set the height of the electrodes we can calculate the current needed and the time to be applied . Considering that gold ions are monovalent:

$$Q = \frac{V \cdot \rho}{m} \cdot F \tag{3.1}$$

Where Q is the charge that flows through the cell to deposit a volume V of gold (density $\rho = 19.3\, g/cm^3$, molar mass $m = 197\, g/mol$) on the cathode, F is the Faraday constant.

This means that to obtain the needed volume we just set the current I and the time t according to $Q = I \cdot t$. The electrodeposition is a superficial process, to obtain the same conditions on the different designs the parameter to keep constant is the current per unit area i. Chosen i, and calculated the volume needed, we calculate time with:

$$t = \frac{V \cdot \rho}{m \cdot i \cdot A} \cdot F \tag{3.2}$$

where A is the base area of the electrode. Results are in table 3.1.

To obtain filled microstructures we need homogeneous ions distribution in the solution. Though, the ions reduced on the gold surface are flowing from the surrounding solution in an anisotropic way, because the electrode is growing in a "hole" (figure 3.4b). Therefore, in the middle of the hole there is a low ions density region. The compensating effect is driven by diffusion with a characteristic time depending on the temperature of the bath. This means that we need to optimize temperature and current taking in account that:

- according with equation 3.1.2, there is a time cost (consider that the used potentiostat could control only 8 channels per time);
- too high temperatures can remove or damage the photoresist layer.

These two parameters were experimentally determined, the temperature was kept between 30°C and 35°C, the current density, was reduced progressively (from $0.07 nA/\mu m^2$ up to $0.015 nA/\mu m^2$), and in many intermediate attempts we obtained hollow pillars (figure 3.7a). These have the advantage of a larger exposed surface, that means a higher capacitance and a lower impedance, according with equation 2.2 this result on an improved voltage recorded.

With $i = 0.015 nA/\mu m^2$ we obtained full pillars (figure 3.7b). When the deposited volume exceed the hole volume (figure 3.4b), the electrode starts growing in the horizontal dimension, with a symmetrical shape, approximatively spherical. The result is a gold mushroom-shaped microelectrodes ($gM\mu Es$), shown in figure 3.7c similar to the one obtained in Spira Laboratory (see section 2.3).

Electrodeposition was performed on a multi-channel potentiostat (VMP3, Bio-Logic Science Instruments, Seyssinet-Pariset, France) using a three-electrode configuration with the MEA electrode

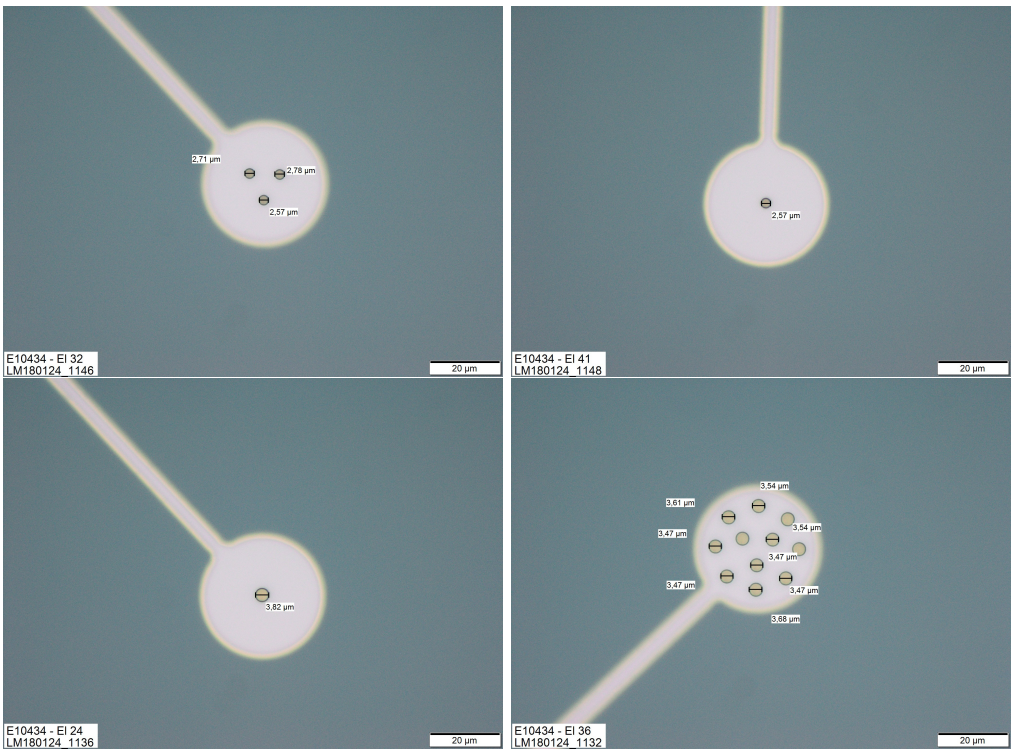

Figure 3.3 – Electrodes images before electroplating obtained with light microscopy (Olympus BX51, Camera: Color View 1)

as working, a Pt mesh as counter and a Ag/AgCl as reference electrode (figure 3.4a). The deposition was performed with galvanic control in a Au electrolyte (NB semiplate AU 100TH).

3.1.3 Electropolymerization

In order to improve their capacitance, the electrodes were coated by electropolymerization with a thin layer of poly(ethylenedioxythiophene)(PEDOT).

Conductive polymer are organic polymers conducting electricity [3, 25], widely used also in biological applications because of their high capacitance [24] (in fact it is a pseudocapacitance because the charge is stored by faradaic processes). PEDOT is a conductive polymer well known and with many applications, used with biological tissue because of his good performance concerning thermal, chemical and most importantly electrochemical stability [37].

Electropolymerization is a straightforward method: the conducting substrate is immersed in a solvent containing the monomer (in this case poly(styrenesulfonate) (PSS)), a potential is applied to reach the oxidation potential of the monomer and the amount of deposited polymer is defined by the duration of maintained potential.

For the same reason of electroplating, the constant parameter on a MEA production is the current per unit area i, that was set to $0.001 nA/\mu m^2$ [1].

Considering charge density for PEDOT is: $Q/V_{PEDOT} \approx 1.4 nC/\mu m^3$ [8], time was calculated to obtain a layer $h_{PEDOT} = 70nm$ thick.

$$t = 1.4\frac{nC}{\mu m^3} \cdot \frac{A_s h_{PEDOT}}{I} = 1.4\frac{nC}{\mu m^3} \cdot \frac{h_{PEDOT}}{i} = 98s \tag{3.3}$$

With A_s surface of the electrode.

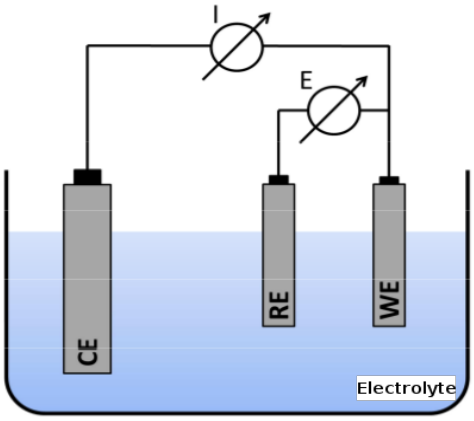

(a) Three-electrode configuration: the CE (Counter Electrode) avoid large reaction happening on the RE (Reference Electrode) that would result in distortion of the voltage difference between RE and WE (Working Electrode)

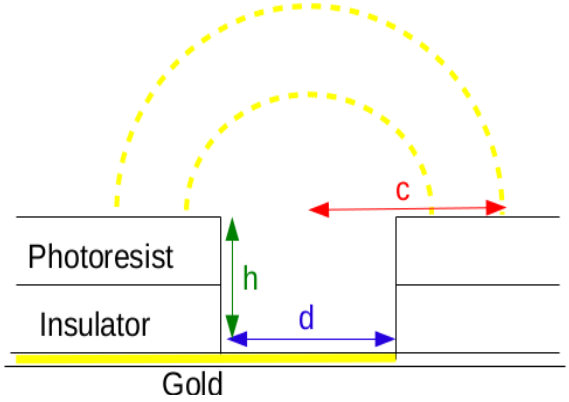

(b) Scheme of the "hole" created by UV-exposure and plasma etching in which the electrodes are growing; $d = 2.7\mu m$ or $3.7\mu m$, $h = 3\mu m$ ($1.5\mu m$ is the photoresist and $1.5\mu m$ the insulator), $c = 2.5\mu m$. The yellow dashed lines give an idea of the growing of the mushroom-shaped electrodes

Figure 3.4

3.2 Characterization of 3D MEAs

3.2.1 Impedance measurements

Impedance spectroscopy is a powerful tool to study the characteristics of an electrode. The idea is to apply a sinusoidal voltage difference between an electrode and a reference, on the same setup illustrated in figure 3.4a and to measure the resulting current.

For a purely capacitive electrode, expressing the sinusoidal voltage in the complex field, $V = V_0 e^{j\omega t}$ where V_0 is the amplitude of the voltage signal, ω the angular frequency and j the imaginary unit. The current response is:

$$I = C\frac{dV}{dt} = jC\omega V \tag{3.4}$$

And the impedance:

$$Z = \frac{V}{I} = \frac{1}{jC\omega} \tag{3.5}$$

For a capacitive electrode the impedance is purely imaginary depending on the frequency, for a resistor it is purely real, in general it is a complex number, depending on the frequency.

Evaluation of the amplitude and phase of the impedance brings informations about performances of the electrode. In our case the impedance is a measure of quality because it influences the signal-to-noise ratio of a recording (as explained in section 2.2)

The impedance at 1kHz is the common reference value for this kind of electrode because of the characteristic frequency on excitable cells signal. These measurements are also an easy way to locate defected electrodes (e.g. broken), when the impedance is 3σ bigger than the mean of electrodes with the same characteristics.

Impedance measurements were performed with a frequency range between $1Hz$ and $10kHz$, with a voltage amplitude of $1V$ on the multi-channel potentiostat (VMP3, Bio-Logic Science Instruments, Seyssinet-Pariset, France), the used electrolyte was PBS.

Impedance measurement were used for different reasons:

- Evaluate the electroplating;
- Evaluate the improvement due to PEDOT coating;

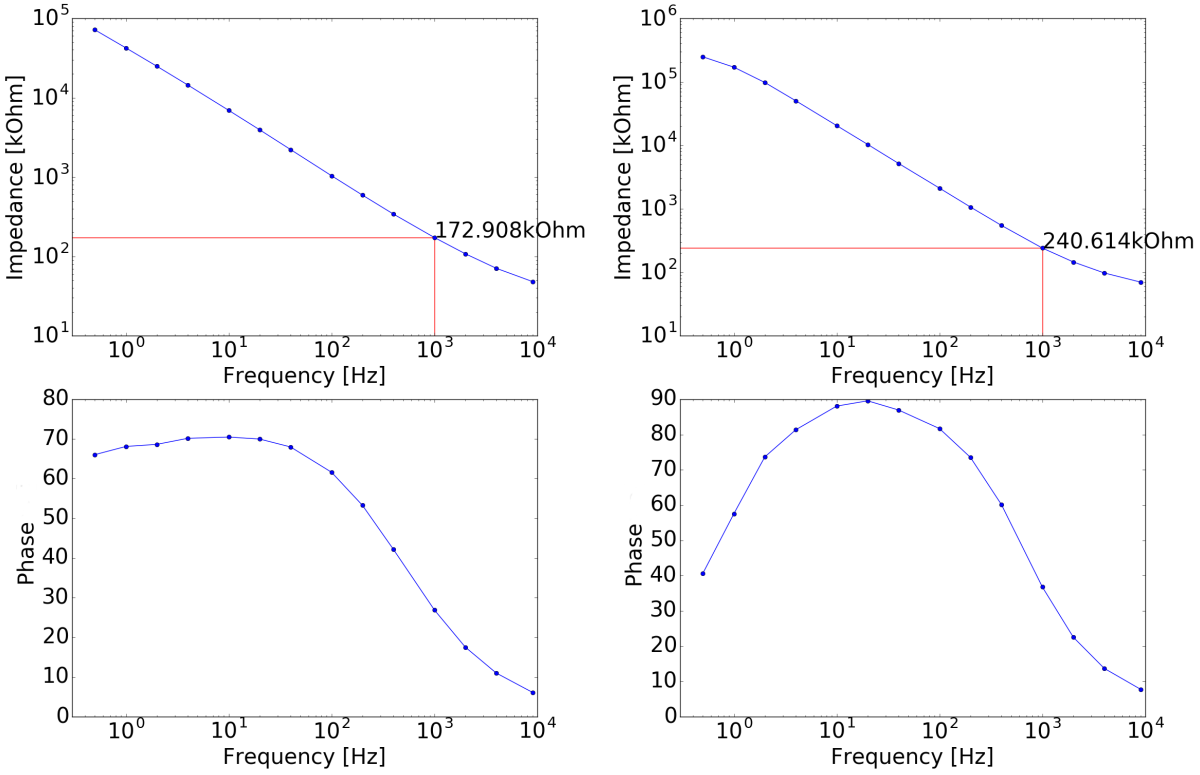

(a) Commercial, planar electrode

(b) Hollow pillar form the 5^{th} row

Figure 3.5 – Impedance and phase spectra for two different electrodes shapes.

- Compare different shapes and designs of electrodes;
- Check the electrodes after several cultures and experiments to see the medium-term stability.

An example of an impedance spectrum is shown in figure 3.5a and 3.5b.

Results after electroplating were coherent with the Cyclic voltammetry (section 3.1.1): when the CV showed a good opening of the hole, impedance was homogeneous with the remaining of the row. Otherwise the impedance was order of magnitude higher (because of the very low area of tiny holes without protrusions).

After the electropolymerization (section 3.1.3) the impedance was, as expected, at least one order of magnitude lower (see figure 3.6). Low enough to be on the same order of the commercial MEAs. Mean values for different electrode shapes are on table 3.2 (electrodes developed by electroplating are listed by row in table 3.2b).

At the end of the experimental work, after several cultures and stimulation experiments, the impedance of every electrode was measured again (see table 3.3). In general it increased by 30-150%. One of the reason is the problematic cleaning of the electrodes. We avoid the use of plasma cleaning or autoclaving on PEDOT because this can be removed by such methods. Still, the result is positive because only 5 % of the electrodes seems to be broken.

3.2.2 Signal to Noise Ratio

The impedance of an electrode is a quality parameter, but it is not taking into account how the cells are interfacing with the electrodes. A more empirical parameter is the signal-to-noise ratio (STR), calculated with spontaneous activity, right before electrical stimulation, as the ratio between the mean amplitude of the signal and the mean amplitude of the noise.

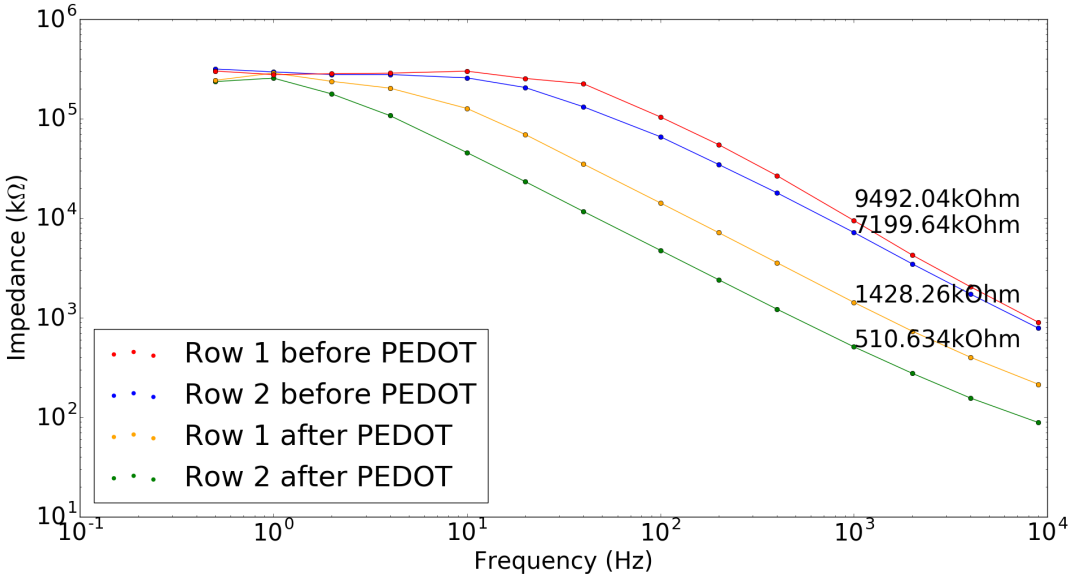

Figure 3.6 – Impedance before and after PEDOT for two electrodes examples

Electrode shape	Mean Impedance (kΩ)
Planar	220 ± 15
Tip	440 ± 60

(a) Average impedance for commercial MEAs

	Mean Impedance (kΩ)		
row	Mushrooms	Hollow Pillars	Pillars
1	340 ± 40	710 ± 55	932 ± 273
2	180 ± 45	358 ± 9	510 ± 16
3	57 ± 8	72 ± 1	91 ± 13
4	240 ± 20	290 ± 20	471 ± 70
5	130 ± 40	246 ± 6	443 ± 66
6	54 ± 1	95 ± 3	120 ± 18

(b) Average impedance after electropolymerization for every electrode shape (columns) and design (rows)

Table 3.2 – Impedance at 1kHz for every electrodes shape.

	Impedance change (relative values) (%)		
row	Mushrooms	Hollow Pillars	Pillars
1	131	201	204
2	112	137	252
3	101	111	194
4	141	158	231
5	119	154	204
6	111	139	171

Table 3.3 – The degradation of impedance, expressed as the ratio of impedance values after and before experiments. The impedance is measured at 1kHz.

It is related with the impedance but it depends also on the cell culture, indeed it is affected by:

- The relative position and surface contact between cell and electrode (that is modifying R_{seal});
- The degree of attachment of the cells (the cleft width), modifying R_{seal};
- The state of health of the cell culture;
- The density and number of layers of cells surrounding the electrodes.

For these reason, the STR is changing in different culture and only the best results are listed in table 3.4.

Electrode shape	Signal-to-noise ratio
Planar	641
Tip	762

(a)

	Signal-to-noise ratio		
row	Mushrooms	Hollow Pillars	Pillars
1	20	235	30
2	36	584	416
3	37	806	288
4	46	631	312
5	51	244	254
6	61	353	278

(b)

Table 3.4 – Signal-to-noise ratio reached with different electrodes.

3.2.3 Scanning Electron Microscopy

Conventional light microscopy is limited to see micrometer sized features because of the relation between the minimal wavelength and resolution of the microscope. An electron microscope instead, uses an electron beam that can reaches very low wavelength and it is therefore suitable for nanometers sized features.

Topographical information about the sample surface are obtained detecting secondary electrons, that are generated as ionization products of the interaction between the beam and the samples. They are emitted very closed to the sample surface because they lose most of their energy in the inelastic scattering with the sample atoms. SEM is furthermore useful to obtain three dimensional-like images tilting the sample, because of the high depth of field .

A Crossbeam Auriga 40 (Zeiss, Germany) was used for SEM to analyze the results of the electroplating (section 3.1.2).

In figure 3.7 some examples are shown.

3.3 Control MEAs

To compare produced MEAs with other shapes and state of the art products, commercial MEAs were used. TiN planar electrodes with $30\mu m$ of diameter (60MEA200/30iR-Ti, Multichannel Systems, Germany) and TiN tip-shaped electrodes (60-3DMEA200/12iR-Ti, Multichannel Systems, Germany) whose structure is shown in figure 3.8.

3.4 Cardiomyocytes

Cardiomyocytes are the cells responsible for the beating of the heart, they are a main part of the myocardium, the heart muscle, embedded in a dense network of collagen and nerve fibers. To provide the level of energy the heart needs for contraction the tissue is highly interspersed with blood vessels and cardiomyocytes contain high amounts of mitochondria.

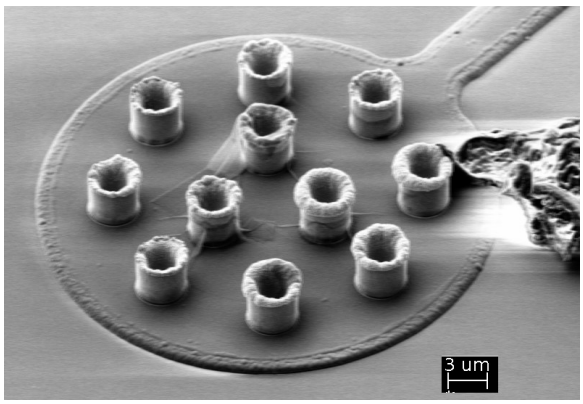

(a) Hollow pillars from 6^{th} row (see table 1.1)

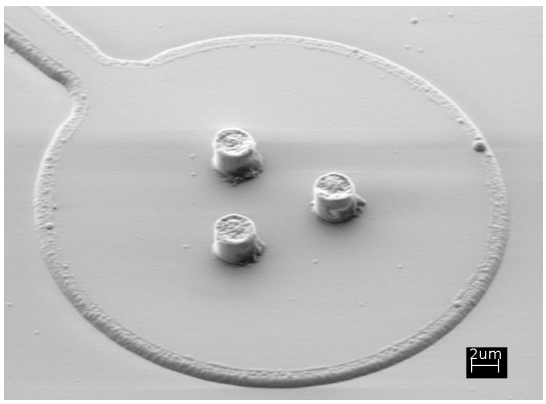

(b) Pillars from 2^{nd} row

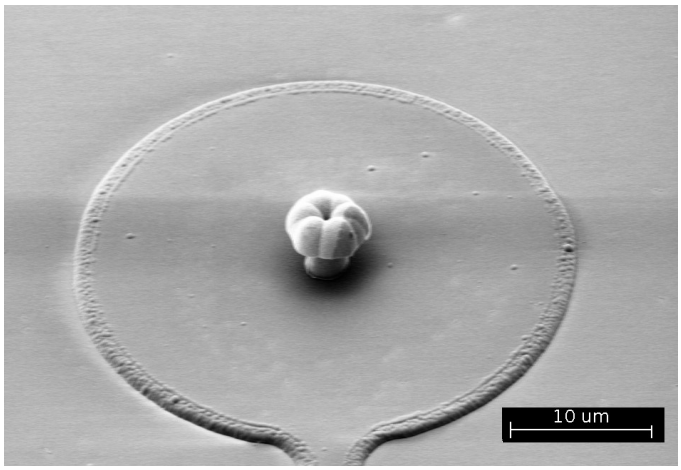

(c) Mushroom-shaped from 1^{st} row

Figure 3.7 – Scanning electron microscopy images of the 3 different type of produced electrodes. Tilting angle 54°.

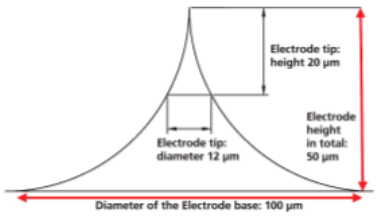

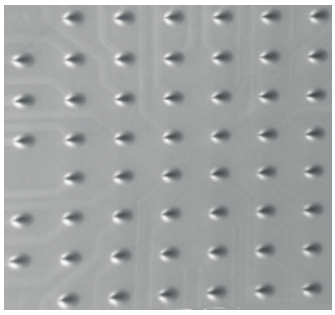

Figure 3.8 – Tip-shaped commercial electrode (60-3DMEA200/12iR-Ti, Multichannel Systems, Germany)

Cardiomyocytes are usually mononuclear, but also cells including two or three nuclei can be found. The connections between these electrically excitable cells are called gap junctions; they consist of specialized intercellular connection creating a direct link between the cytoplasms, allowing the passage of particular molecules, ions and electrically impulses.

Cardiac muscle fibers show a branched, highly interconnected structure and a large amount of gap junctions providing the rapid conduction of electrical signals throughout the myocardium which therefore is able to act as functional syncytium. In this syncytium, cells are electrically synchronized allowing the myocardium to act as a single contractile unit.

As already suggested, an electrical signal is responsible of the contraction of the heart, it is called action potential, as in neurons even though it exhibits a different shape, involving different

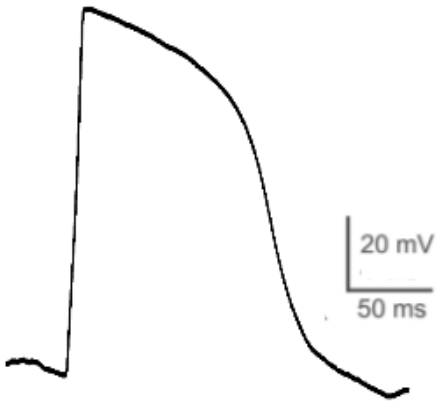

Figure 3.9 – Cardiomyocyte action potential measured with patch-clamp electrode. Data courtesy to Dr. Udo Kraushar (NMI)

ion channels.

The cardiomyocytes action potential, shown in figure 3.9 is characterized by a resting potential of about -85mV, that rises to about +20mV, during each beat. After the initial spike, the membrane remains depolarized for about 0.2 second, exhibiting a plateau, followed at the end of the plateau by abrupt repolarization. The first, fast depolarization is due to the opening of voltage gated fast sodium channels, that are also rapidly closed (1-2ms); on the same time, calcium-sodium channels are activated, slower in the opening but even in the closing, they allow for tenths of seconds the flowing of sodium and calcium ions, these lasts being responsible of the activation of the contracting process. When these channels are closed the potassium membrane permeability increases rapidly and the repolarization occur [31].

Cardiomyocytes are often the first cells used to test new electrophysiolgy experimental tools (e.g. the first MEA [32]), because they are relatively big, easy to cultivate, they grow in a very dense layer, and the action potentials is almost simultaneous on the whole culture. On a MEA setup it is easy to record activity in many electrodes on the same time, to see without particular data analysis differences between electrodes and changes in the culture behavior (beating rate changes, beating amplitude changes) that can for example be induced by excessive stimulation.

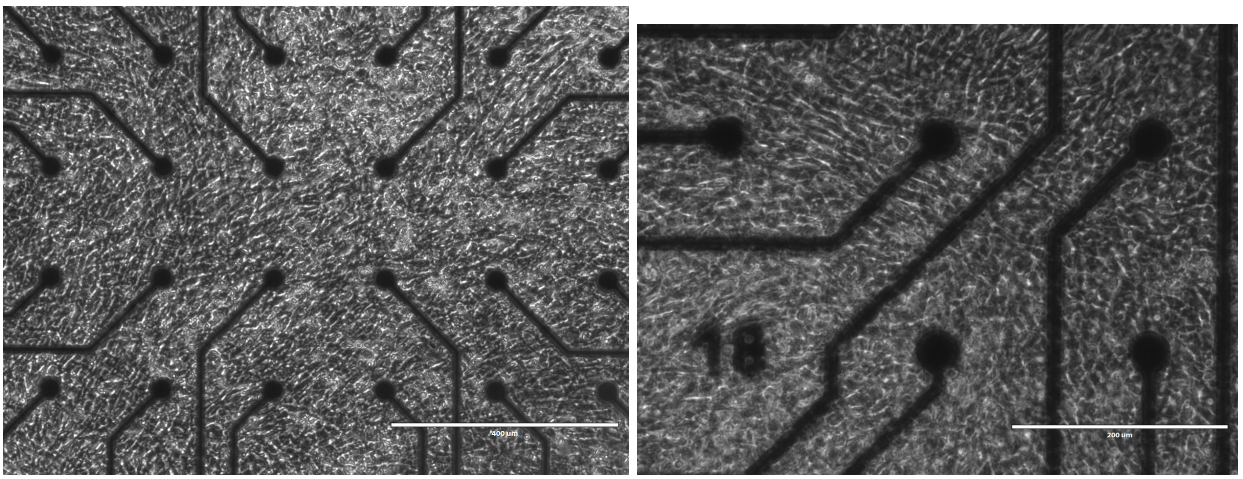

Figure 3.10 – Microscope images of a cardiomyocytes culture on a MEA on DIV 5

3.4.1 Cell culture

The experimental procedures were carried out in compliance with the institutional guidelines of the NMI (Regierungspräsidium Tübingen). The preparation of cardiomyocytes was based on earlier reports [5]. Cardiac myocytes were prepared by enzymatic dissociation from 13-day chick embryos. Hearts were removed, ventricles finely minced and dissociated in 4-5 cycles of trypsin at 37°C. Discarded the remaining coarse component, the cells were diluted in a FBS 20% medium with a density of $20000\,cells/\mu l$. Finally they were plated on MEAs, previously sterilized with 70% Ethanol overnight and coated with $6\mu l$ of nitrocellulose (5% diluted in methanol). The cells concentration ensure a good covering, trying to obtain a single layer of cells. Cells cultures were incubated at 37°C and 5% CO2. The medium was changed every 2-3 days. Experiments started after five days in vitro (figure 3.10).

Chapter 4

Experiments and results

4.1 Overview of different electrodes

To clearly understand the following discussions it is worth to have an overview on the different electrodes used in the experiments:

- Planar electrodes on commercial MEAs (see section 3.3), we refer to them as "planar";
- Tip-shaped electrodes on commercial MEAs (see section 3.3), we refer to them as "tips";
- Solid pillars-shaped electrodes obtained by electroplating (see section 3.1.2), we refer to them as "pillars";
- Hollow pillars-shaped electrodes obtained by electroplating, we refer to them as "hollow pillars" ("h_pill" in the figures);
- Mushroom-shaped electrodes obtained by electroplating, we refer to them as "mushrooms";

Consider, furthermore, that on the electroplated MEAs the number of protrusion for every electrode is changing (see section 1.2). This is the reason why in many cases we refer to the row of considered electrodes.

In part of the analysis we tried to find features related with the electrodes shape and not the design, also because to compare different designs too many experiments were needed.

4.1.1 Characterization of recorded signals

Extracellular recording of cardiomyocytes action potential (extracellular AP) were recorded on every type of electrode with a frequency around $1.3Hz$. The signal-to-noise ratio of the extracellular recording for each electrode was analyzed in section 3.2.2.

After identification of electrodes with reliable spontaneous extracellular AP, stimulation electrodes were selected. Upon application of strong electrical pulses, we often obtained a switching of the signal between an extracellular AP and in-cell like recording of action potential (in-cell AP) - see section 2.1.3. This phenomenon is believed to be attributed to electroporation (see section 2.4).

The conditions that lead to obtain such a recording are discussed in the following sections, but we need first of all to develop a method to discriminate between these two different recordings.

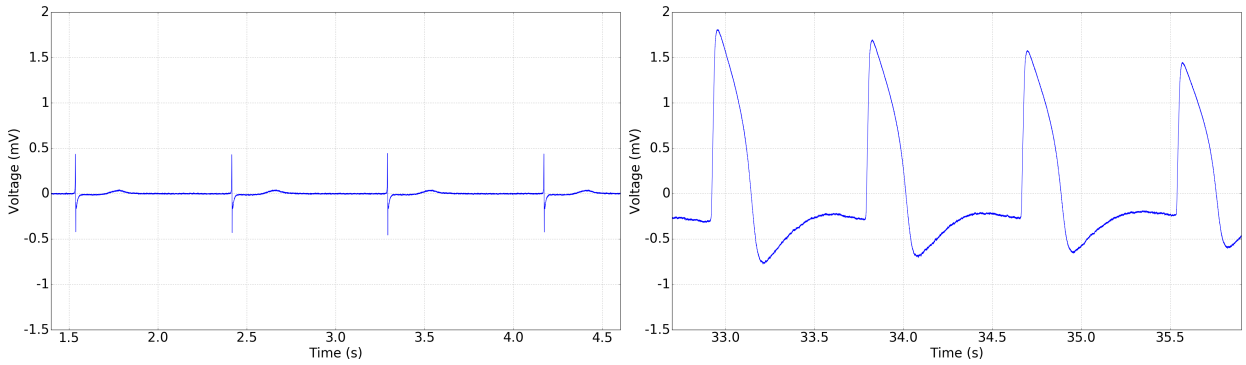

(a) Before stimulation, extracellular recording

(b) After stimulation, the electroporation give access to in-cell recording

Figure 4.1 – Cardiomyocytes action potential recorded with hollow pillars electrodes (row 3)

The characterization of the switching can be described as following:

- the shape of the signal is modified. In-cell AP (fig 4.1b) is monopolar. Extracellular AP (fig 4.1a) can be biphasic with a sharp peak at the beginning, a stable phase at the resting potential and a final small bump, after around 400 ms corresponding to the repolarization of the cell;
- in-cell APs amplitude is in the order of $1 - 10mV$, the extracellular amplitude is in the order of $50\mu V - 2mV$; consider that an intracellular patch recording ranges between -90mV and 40mV.

These changes between extracellular signal and in-cell signal is evident on every shape of electrode, even though the AP shape and amplitude are different between different culture and electrodes. Common differences are:

- extracellular AP can be biphasic or monophasic, depending on the relative position between the reference electrode and the flow of the contraction along the cell culture (see the difference between fig 4.1a and fig 4.2a);
- the small bump that ends an extracellular AP can be pretty evident or very little defined (see fig 4.1a and fig 4.2c);
- extracellular sharp peak can be still present in the in-cell AP (fig 4.2d). In some cases the membrane conductance is probably not high enough to neglect the first term in equation 2.2. In many cases the electrodes are not in contact with a single cell, because the cardiomyocytes are forming a dense layer of cells; therefore the electroporation is probably involving only one of the cells in contact with the electrodes and we still see the extracellular AP of the others. Furthermore, we cannot ensure that the we have strictly one layer of cells on the whole culture, so the extracellular sharp peak can be the summation of many cells in different positions.

The latter is the reason why the AP amplitude is not a good parameter to define the presence of an in-cell recording.

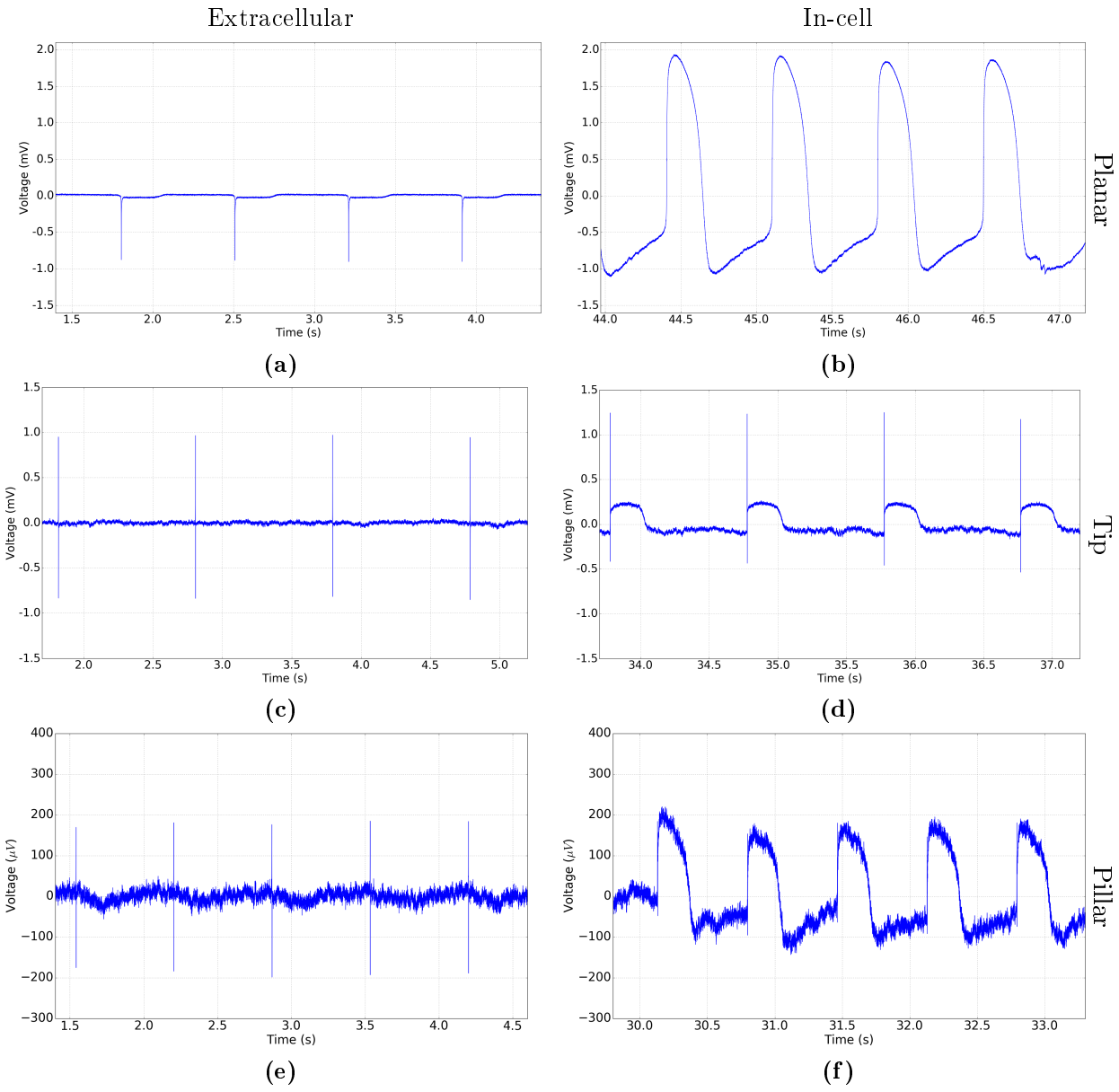

Figure 4.2 – Extracellular (**(a,c,e)**) and in-cell (**(b,d,f)**) signal for a planar electrode (**(a)**, **(b)**), a tip-shaped electrode (**(c)**, **(d)**) and a pillar electrode (**(e)**, **(f)**). The change in the signal shape was obtained upon electrical stimulation.

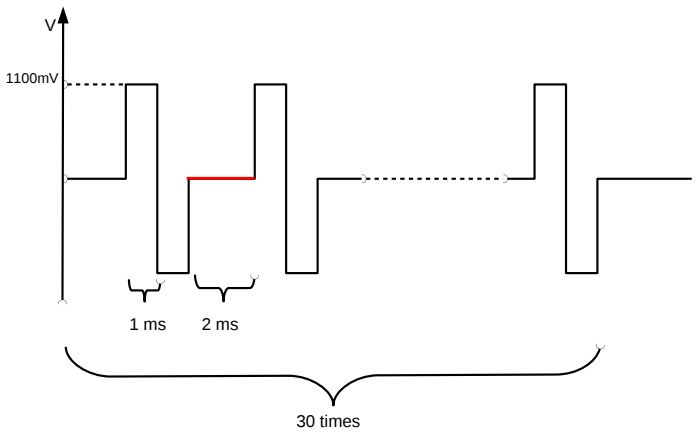

Figure 4.3 – Voltage pulses used to compare electrodes performances on electroporation

4.1.2 Electrical stimulus for in-cell signals

Stimulation electrodes were always selected after identification of reliable spontaneous signals on these electrodes. Based on literature parameters [2, 11], many different stimuli were tested varying the frequency, peak-to-peak amplitude, number of repetitions and the time in between two repetition (red in fig 4.3). Finally a stimulus with good efficiency and mostly not harmful for the cells (cells are alive over a period of days and no sensible difference between before and after the electroporation is shown), was selected as the standard voltage stimulus used to obtain in-cell recordings in order to compare electrodes performances. The "standard stimulus" was biphasic with an amplitude of $2.2V_{p-p}$, repeated 30 times with a frequency of 250Hz (fig 4.3)

4.1.3 Experimental protocols

Three different experiments were designed to highlight the electrodes features.

1. The standard stimulus applied to a large number of cells. The goal of this experiment was to compare the in-cell recording duration obtained on different electrode types.

2. The voltage of the standard stimulus was varied by steps of 200 mV ranging from 100 mV to 1.6 V, looking for the threshold that causes the electroporation (at low voltages the stimulus has no apparent consequences). A lower stimulation voltage would result in a smaller cells physiology alteration.

3. Stimulation was repeated onto the same cell over a period of minutes and hours to see if the repeatability was the same on all the electrode types. The repeatability is fundamental for drug screening over long periods.

In all the protocols further stimulations were performed only after complete recovery to the pre-stimulus conditions (beating and amplitude), a recovery period of 2 minutes was usually sufficient. In some experiments we stimulated more than one cell per time, chosing distant electrodes and without exceeding three on the same time, indeed the current flow is not delimited to the single electrode.

4.2 Evaluation of in-cell recordings

Data analysis was performed with an entirely custom-developed software using Python.

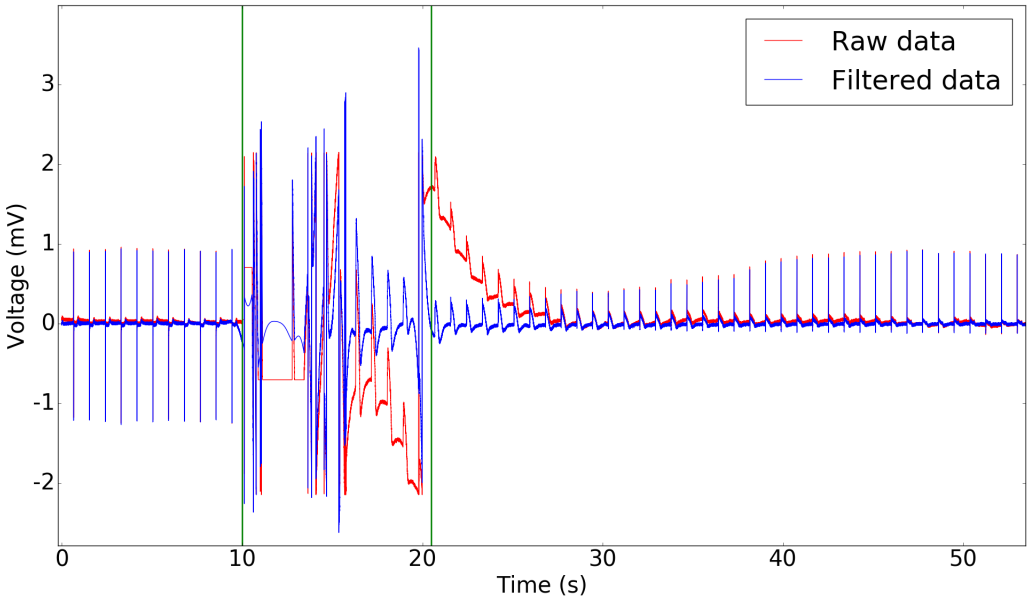

Figure 4.4 – Raw (red) data filtered (blue) with a high-pass filter (cut-off frequency of 0.8 Hz). The green vertical bars show the neglected interval for the analysis

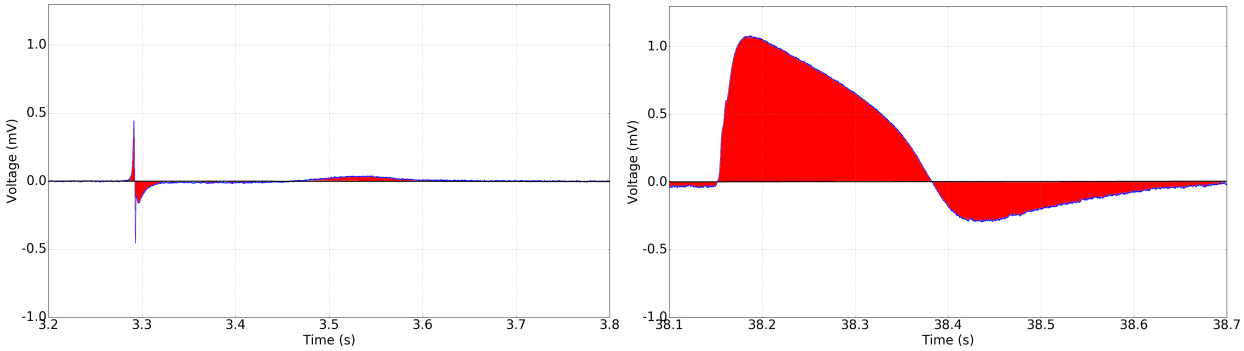

Figure 4.5 – In red the Area Under the Curve, for an extracellular AP (left) and for an in-cell AP (right)

First of all a Butterworth high-pass filter of the second order with a cut-off frequency of 0.8 Hz was applied to the data, to reduce the stimulus artifact (figure 4.4). A manually defined interval (around 10s), comprising stimulation and subsequent artifact, was removed from the analysis (green bars in figure 4.4).

Reversible electroporation is useful because the cell is not damaged but the membrane recovers in a short time. The recovery is characterized by stable extracellular signals. It is fundamental to define a parameter that can discriminate between the normal state (extracellular AP) and the in-cell state (in-cell AP). As mentioned in section 4.1.1, the AP amplitude is not a good parameter because there are many cases in which the amplitude is not changing even if the shape of the AP is clearly changed (see figure 4.5). Instead the area of the voltage signal is enhanced by electroporation, because of the changing in the shape.

The Area Under the Curve (AUC), shown in figure 4.5, expressed as the ratio between the mean area after and before the stimulus, will be the basic parameter for the following analysis.

After computing the AUC for every peak, a threshold of 2 was set to define whether or not the cell was electroporated. When a cell was detected as electroporated, AUC time variations were analyzed: after electroporation AUC reach values up to 100, and then decrease with an exponential

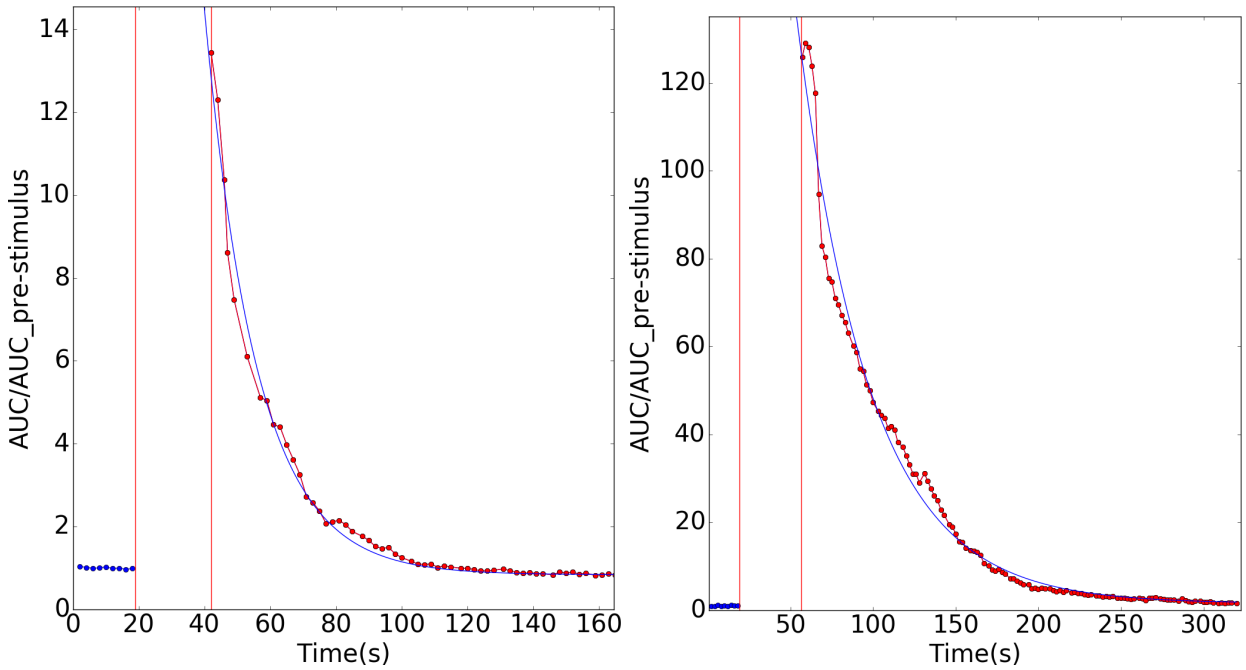

Figure 4.6 – Examples of the recovering process from the in-cell recording, in blue the exponentials fitting curves (equation 4.1)

slope, because of the membrane repair dynamic [11] (figure fig 4.6).

The curves were fitted with the following exponential function:

$$AUC(t) = Ae^{-\frac{t}{\tau}} + 1 \tag{4.1}$$

2τ is the parameter used in the following analysis to evaluate the duration of the in cell recording.

4.2.1 Duration

As explained, the chosen parameter to evaluate the duration of the in-cell recording was 2τ. It is calculated for every experiment in which the standard stimulus (section 4.1.2) was applied. The results are grouped by shape in the violin plot of figure 4.7 without taking into account the different row designs. The arithmetic mean (purple dots in the figure) for every shape is calculated after removing:

- the outliers, values more than 3σ from the mean (red dots in the figure);
- the zeros, experiments in which the electroporation was not obtained.

In table 4.1a the mean values are listed for every shape.

No substantial difference are visible, and all the means are compatible one another. Hollow pillars show the higher value (table 4.1a), but this could be related to the high impedance of some rows, it is worth to have a closer look: the results detailed by row are on table 4.1b, the mean impedance for every row is shown.

The simple explanation of this little difference is the improved impedance, results in a higher current and stronger stimulation of the cells.

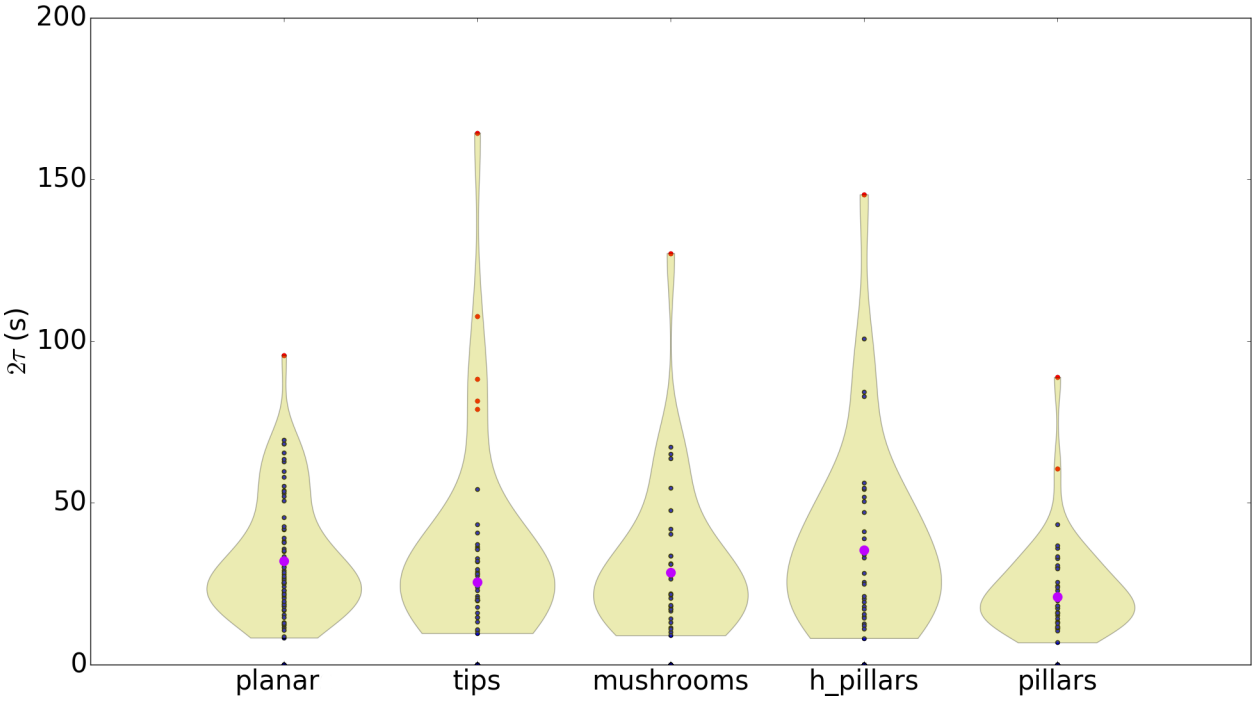

Figure 4.7 – Violin plot: the duration of the in-cell recording after the standard stimulation is plotted for every shape of electrodes (blue dots). The outer shape shows an empirical representation of the probability distribution of the data (mirrored). Red dots are outliers not taken into account for the mean calculation (purple dots).

Electrode shape	N	Mean 2τ (s)
Planar	70	31 ± 16
Tip	37	28 ± 16
Pillar	41	21 ± 8
h_pillar	34	35 ± 22
Mushroom	32	26 ± 10

(a) Average 2τ for different shapes. N is the number of averaged data.

row	N	Mean 2τ (s)	Mean impedance (kΩ)
1	2	20	340 ± 40
2	6	27	180 ± 50
3	14	43	57 ± 8
4	7	34	240 ± 20

(b) Relation between 2τ and impedance for hollow pillars. It is not statistically valuable (N is too low), but it shows that in general lower impedance gives a longer in-cell recording

Table 4.1 – Duration of the in-cell recording

Electrode type	N	Threshold (mV)
Planar	30	750 ± 320
Tip	29	560 ± 380
Pillar	21	870 ± 280
h_pillar	34	950 ± 350
Mushroom	21	930 ± 250

Table 4.2 – Mean voltage threshold inducing electroporation for different electrode shapes

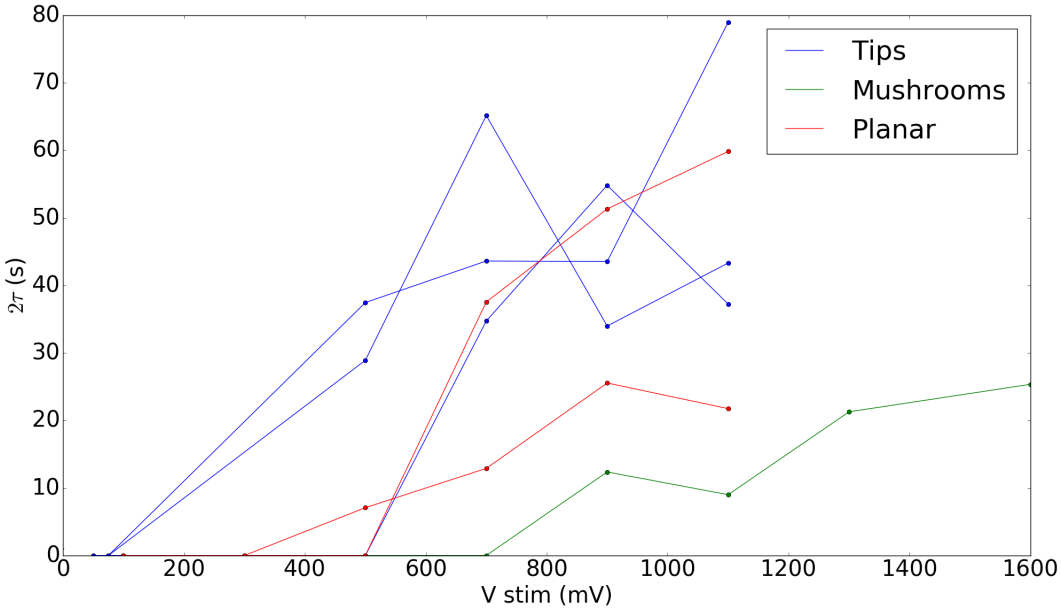

Figure 4.8 – The duration of the in-cell recording (y-axis) is increasing with the amplitude of the electrical stimulation (x-axis). The experiment was repeated with three different electrode type.

4.2.2 Stimulation threshold

As explained in section 4.1.3, in the second experiment we searched for the stimulation voltage that induce electroporation. First we verified that the threshold exists: starting with a voltage of 100 mV (that never triggered electroporation), then repeating the stimulation increasing the voltage, electroporation was induced at some point. Successful electroporation was confirmed by visual inspection of the signal shapes. Further increasing of the voltage induced always electroporation. Decreasing the stimulation voltage below threshold did not lead to in-cell like signal shapes. The step size of the stimulation threshold was 200 mV.

For every shape the mean of that threshold is listed in table 4.2.

The increasing response to voltage steps is shown for some example in figure 4.8.

Although with a big standard deviation, tip-shaped electrodes seems to more easily induce electroporation. However the large standard deviation prevents a statistical comparison.

Since R_{seal} is an important parameter for the electrical coupling (see section 2.1.2) it should directly influence the amplitude of the extracellular recordings, increasing the signal the more is the contact surface [12, 16]. As explained in section 3.2.2, this should be the main explanation for the variability of the recorded signal within the same cell culture: the signal in each electrode is depending on how much of the cell is in contact with it. The best contact surface would result from an engulfing of the 3D electrode.

A good electrical coupling should also increase the transmembrane electric field induced by the

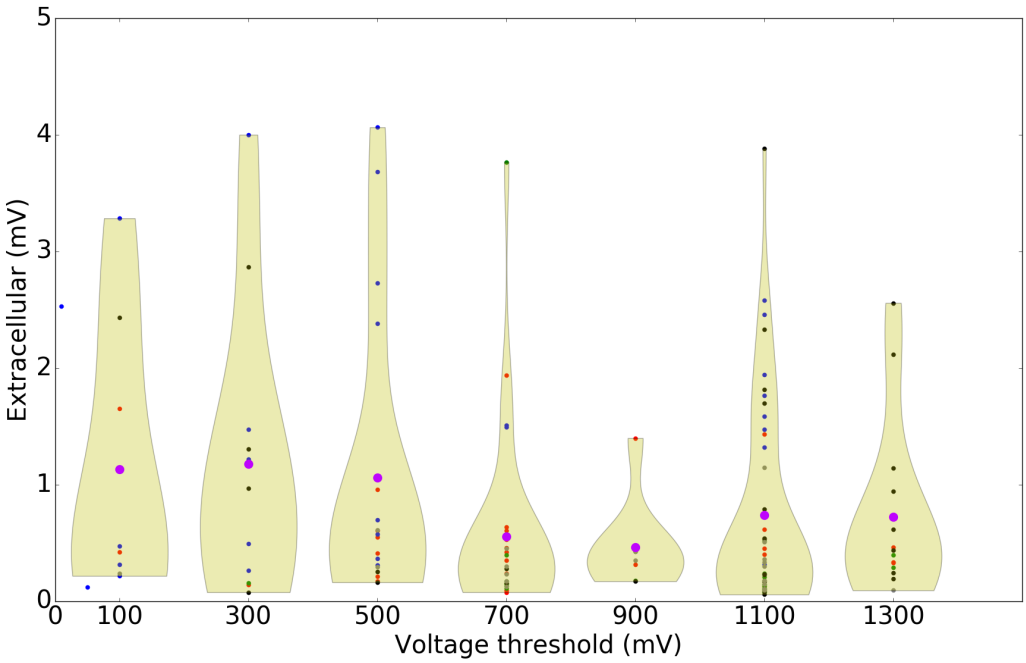

Figure 4.9 – The extracellular AP amplitude (y-axis) before electrical stimulation should be directly influenced by R_{seal}, the principle parameter for electrical coupling. The voltage threshold (x-axis) should be a direct consequence of the transmembrane electric field. Different colors show different shapes. The purple dots represent the extracellular mean.

stimulation, responsible for electroporation [38]. Therefore we would expect corresponding to bigger extracellular recordings, a low voltage threshold for electroporation. The analysis of this aspect is shown in figure 4.9 with different colors for every different electrode shape.

Surprisingly, it seems that the extracellular recording amplitude is not related with the transmembrane electric field. This suggest to consider the other components influencing the extracellular signal (see section 3.2.2) such the fact that cardiomyocytes are so tightly connected, that the extracellular signal is not only depending on the single R_{seal}, but on a multiple cell interaction, that could even be influenced by multilayer of cells.

4.2.3 Repeatability

The third experiment type was focused on the repeatability of the electroporation protocol over minutes and hours (section 4.1.3). Three different experiments are shown: repetitions every 10 minutes (4.10a), every 20 minutes (4.10b) and every hour (4.10c).

It is clear that there is no difference between different electrode shape. Nevertheless this shows that the stimulation is repeatable with similar effects in many cases with all the electrodes tested and over a period of hours. Though, if the voltage is not far from the threshold, the same stimulus can induce electroporation in some cases and not in others.

When the voltage stimulus is higher enough than the threshold (i.e. the electroporation duration is significant), the repetition lead to the same effects (with the characteristic variability already seen in the previous sections), showing that the cells are completely recovering in 10 minutes in all the tested electrodes.

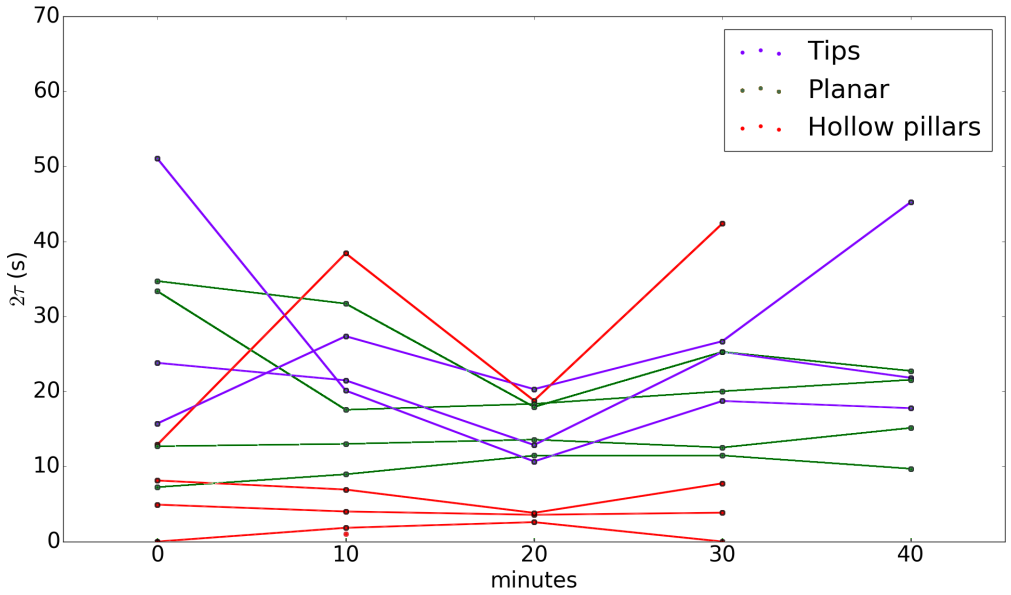

(a) Electrical stimulus repeated every 10 minutes

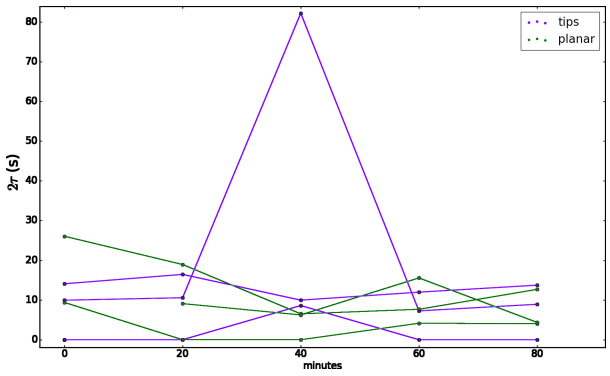

(b) Electrical stimulus repeated every 20 minutes

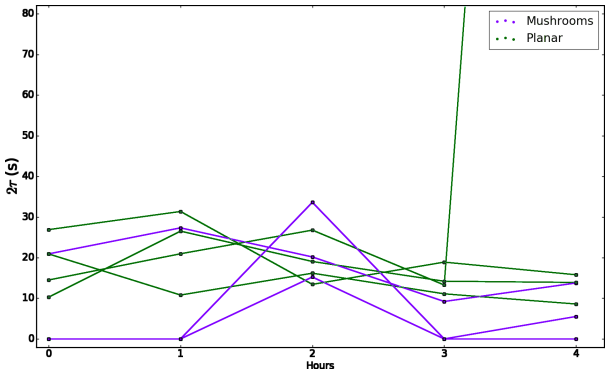

(c) Electrical stimulus repeated every 60 minutes

Figure 4.10 – Repeatability of the electroporation protocol over 10, 20 and 60 minutes. a) shows that in ten minutes the cells are already back to the pre-stimulus conditions while b) and c) show that electroporation can be used for long term cells screening.

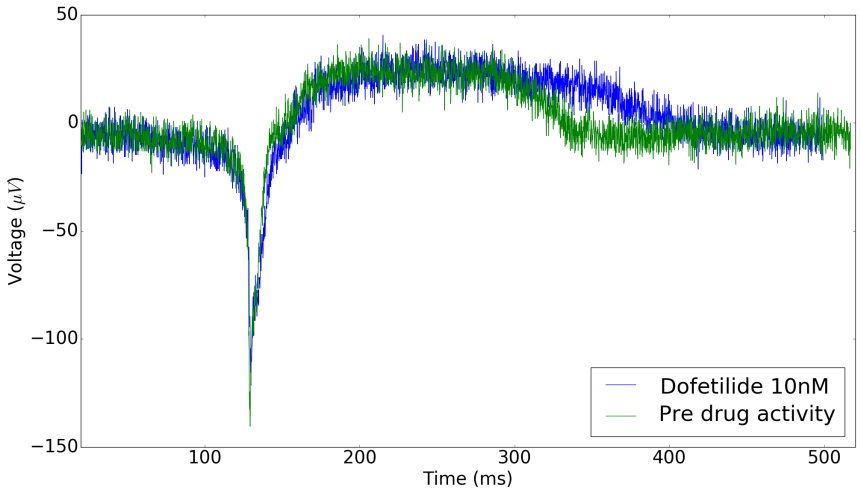

Figure 4.11 – The green data is the spontaneous in-cell recording obtained over a period of days. In blue is the effect of Dofetilide with a 10nM concentration in the culture medium.

4.3 Spontaneous in-cell recording

On one culture a spontaneous in-cell recording was obtained: without any electrical stimulus the recorded signal had the shape of an in-cell recording (even if only in the order of microvolts) over a period of days.

This could be accounted to a tight engulfment [12], a partial physical explanation is in the second term of equation 2.2: the engulfment reduce the conductance of the cleft between cell and electrode. One other possible contribution is the recruitment of voltage independent ionic channels or the formation of nanopores within the confined region of the junctional membrane that enhance the conductance. Both mechanisms can be triggered by the curvature of the membrane along the $gM\mu E$ cap and stalk [22, 40].

To show the utility of this recording, we applied dofetilide, an antiarrhythmic agent, with a 10nM concentration in the cell medium. It is known that dofetilide broaden the cardiomyocytes action potential [2]. The effect is evident in figure 4.11. It is difficult and can be impossible to show the same effect with an extracellular signal, consider indeed that sometimes the “bump” marking the end of the AP is almost invisible (section 4.1.1, figure 4.2c).

4.4 Staining attempt

To have a better understanding of the process and to have some proof that electroporation is the mechanism inducing the in-cell recordings a staining experiments was designed. Three different dyes were used:

- Propidium iodide (PI) (Thermo Fisher Scientific), added to the cell culture before electrical stimulation. It is a fluorescent dye (emitting in the red spectrum) that binds to double-strand DNA. It cannot cross intact plasma membrane;
- DAPI (4',6-diamidino-2-phenylindole, Thermo Fisher Scientific), added after electrical stimulation. A dye (emitting in the blue spectrum) binding to the cells DNA that can cross intact cells membranes;
- Yo-pro®-1 (Thermo Fisher Scientific) added after electrical stimulation. A dye (emitting in the green spectrum) used as a marker for apoptosis processes.

Fluorescence is detected with Spinning Disc Confocal Microscope (Zeiss, Oberkochen, Germany).

Electroporated cells should be marked by PI [2]. Yo-pro®-1 should mark cells dying after the electrical stimulus, it should help distinguishing electroporated cells and dying cells. DAPI marks all the cells nuclei, it is useful to neglect background staining: if there is no blue staining on a red or green patch, it is probably not a cell, but only a background.

The images resulting from the staining experiment are shown in figure 4.12. There are no red (PI) stained cells near the electrodes that shown in-cell recordings after electrical stimulation. The reason is probably that cardiomyocytes are forming a so dense layer, the syncytium (see section 3.4), that PI cannot flow under the cells - consider that the nano holes induced by electroporation are in the membrane between the cell and the electrode. The same negative result was obtained in two other attempts.

Nevertheless, the staining was clear for DAPI and Yo-Pro®-1, identifying all cells nuclei (blue), dead cells (red) and dead or dying cells by apoptosys (green).

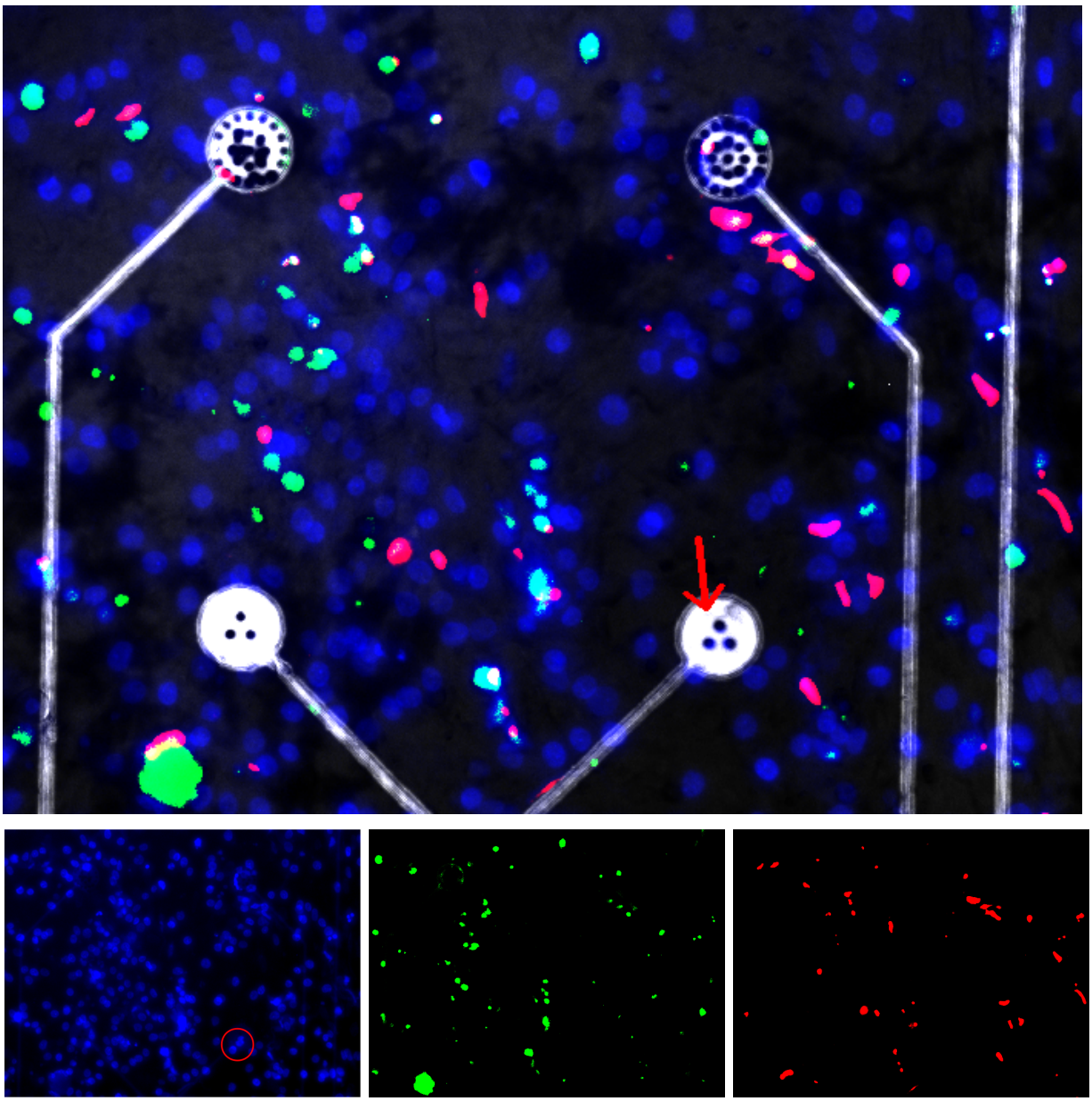

Figure 4.12 – Cardiomyocytes culture stained with DAPI (blue), Propidium Iodide (red) and Yo-Pro®-1 (green): the red arrow is pointing at the electrode that was stimulated and had an in-cell recording, no PI (red) was visible on the cells over that electrode (red circle on DAPI (blue) spectrum).

Chapter 5

Discussion and conclusion

5.1 Discussion

In this work **in-cell** recordings have been performed upon electrical stimulation using various three-dimensional electrodes. This phenomenon is believed to be attributed to electroporation and has been used several times in recent years [36, 11, 2]. Braeken *et al.* used CMOS-MEAs with $1.2\mu m$ three dimensional hexagonal electrodes, and the stimulation protocol was based on a $10Hz$ biphasic pulse with a peak to peak amplitude of $3.3V$ [2]. In contrast Xie *et al.* successfully applied MEAs with nanopillars (tip radius $< 100nm$), and the stimulation protocol was based on a $20Hz$ biphasic pulse with a peak to peak amplitude of $2.5V$ [36]. Spira *et al.* used gold mushroom-shaped microelectrodes with a cap diameter of $1.5\mu m$, and the stimulation protocol was based on a positive square pulse lasting $50 - 100ms$ with an amplitude of $1 - 2V$ [11]. These three studies were all performed on cardiomyocytes -from different animals- but had different electrode materials, electrode shapes and stimulation protocols. Taken together they indicate that electrode geometry, material and even stimulation protocol may not be the decisive factor to obtain transient in-cell like recordings. Indeed, in our work we analyzed if the electrode shape is affecting the electroporation physiology, using PEDOT coated gold structures -pillar, hollow pillar and mushroom shaped- and TiN tip shaped electrodes as well as planar, two dimensional TiN electrodes. The electrical stimulus had a frequency of $250Hz$ lasting $120ms$ with an amplitude of $2.2V_{p-p}$.

The most likely **mechanism** for the occurrence of in-cell signals are transient pores in the cell membrane, caused by the electric pulses, even though we were not able to conclusively demonstrate electroporation using fluorescent markers (section 4.4). The investigated cells always recovered from electroporation and there was no evidence of irreversible cell damage caused by the electrical stimulation. This result is in line with an early report on bi-stable recordings from leech neurons [14], and with the literature cited above. One major challenge when analyzing the performance of 3D electrodes for in-cell recordings is the knowledge of the effective transmembrane voltage across the cell membrane under consideration. Even within the same cell culture on MEAs, the same stimulus applied has different effects depending on the relative position between cell and electrode. The uncertainty about the effective transmembrane voltage induced by electrical stimulation is probably the reason for the large standard deviation on duration and threshold experiments (sections 4.2.1 and 4.2.2) and for the choice of the approach: most of the experiments were designed to be repeated many times with the purpose to obtain information from the statistics analysis. More than 500 electrical stimuli were applied and the effect analyzed.

The **duration** of the in-cell recording depends on the recovery of the cell membrane as studied by Hai and Spira [11]. Two main processes were considered by the authors as responsible for the membrane repair process: one fast process when Ca^{2+} influx through the injury site triggers the fusion of pre-existing intracellular vescicles within the plasma membrane, and one smooth process, in which the calcium-induced vescicle exocytosis reduces the plasma membrane tension and thereby enables pore repair by constriction and bilayer resealing. This could explain why there is no relationship between the amplitude of the in-cell signal and the recovery time (not shown): large holes in the membrane could induce a faster resealing mechanism. In this work we showed

that the duration of the in-cell recording doesn't change with the shape of the electrode protrusions neither with the dimensionality: planar and 3D structured electrodes gives comparable results (section 4.2.1). This does not mean that the membrane is damaged on the same way, but that the recovering process may occur with similar time scale.

On tip-shaped electrodes, it was easier to obtain electroporation in the sense that a lower **voltage threshold** was needed (section 4.2.2). The interpretation is simple: the edge of the tip is nanometric so in that point there is a higher electric field giving locally a larger transmembrane electric field. This advantage suggest to deepen the study of nanostructures but it seems not confirmed by Xie et al. electrical stimulus choice [36] since on nanometric tips they used a stimulation voltage of $2.5V_{p-p}$.

One aspect that could not be investigated in this work is the one-to-one correspondence between cell and electrode, because cardiomyocytes are acting as a single unit (see section 3.4). This could be a reason to prefer 3D structures for the using of electroporation protocols when applied on other cell type.

Finally, a **spontaneous in-cell recording** was obtained (section 4.3), similarly to studies from Spira's lab [12]. It is an important result, because it was obtained in the past, only with Aplysia neurons [28, 9] (see section 2.3), even if the amplitude of the signal is small and it remains to prove that it can be repeated. An explanation of the in-cell shape with a small amplitude would be that we obtained only one of the two requirement indicated by Spira for an in-cell spontaneous recording. As explained in section 4.3 a tight engulfment would increase R_{seal} and G_{leak}. Given the large dimensions of our mushrooms and the small amplitude of the signal we believe that there is no engulfing and therefore R_{seal} is small. G_{leak}, responsible of the in-cell shape, is large. Further investigation of this theory would be the opportunity to separate the two effects, always obtained together in the past. Increasing G_{leak} could be related to the curvature or the roughness of the electrode surface. This approach would be completely new for the research on three-dimensional microstructures: the study of the effects of curvature and surface roughness on the cell-electrode coupling.

5.2 Conclusion

The aim of this work was to develop three-dimensional microstructures on MEAs to record signal from electrogenic cells. All the designed microstructures were successfully used, with impedance and signal-to-noise ratio comparable with commercial MEAs (sections 3.2.1 and 3.2.2) and were still functional after tens of cultures and experiments.

MEAs were tested on cardiomyocytes cell cultures (section 3.4.1) allowing measurements and electrical stimulation over days, proving a good biocompatibility. Electroporation protocols were developed (section 4.1.2) giving access to in-cell recordings -without damaging the cells- repeatedly over a period of hours (section 4.2.3).

The comparison between different electrode shapes did not show relevant differences on the duration of the induced in-cell recording (section 4.2.1). Electroporation was easier to obtain on tip-shaped electrodes, suggesting further studies on nanostructured electrodes (section 4.2.2).

The main information coming from this study is that there is no evident reason to apply electroporation with three-dimensional microstructures. Electroporation was obtained using planar commercial MEAs with exactly the same protocol used for three-dimensional electrodes, with comparable results and without damaging the cells. The use of such a technique on three-dimensional electrodes would be justified only by drastic difference, such a much lower voltage needed to electroporate the cells -this would result in a lower alteration of the culture physiology.

Bibliography

[1] Johan Bobacka, Andrzej Lewenstam, and Ari Ivaska. "Electrochemical impedance spectroscopy of oxidized poly (3, 4-ethylenedioxythiophene) film electrodes in aqueous solutions". *Journal of Electroanalytical Chemistry* 489.1-2 (2000), pp. 17–27.

[2] Dries Braeken et al. "Open-cell recording of action potentials using active electrode arrays". *Lab on a chip* 12.21 (2012), pp. 4397–4402.

[3] Chwan K Chiang et al. "Electrical conductivity in doped polyacetylene". *Physical review letters* 39.17 (1977), p. 1098.

[4] Ariel Cohen et al. "Reversible transition of extracellular field potential recordings to intracellular recordings of action potentials generated by neurons grown on transistors". *Biosensors and Bioelectronics* 23.6 (2008), pp. 811–819.

[5] P Connolly et al. "An extracellular microelectrode array for monitoring electrogenic cells in culture". *Biosensors and Bioelectronics* 5.3 (1990), pp. 223–234.

[6] Xiaojie Duan et al. "Intracellular recordings of action potentials by an extracellular nanoscale field-effect transistor". *Nature nanotechnology* 7.3 (2012), p. 174.

[7] Peter Fromherz. "The neuron-semiconductor interface". *Bioelectronics-from theory to applications* (2005), pp. 339–394.

[8] Ramona Gerwig et al. "PEDOT–CNT composite microelectrodes for recording and electrostimulation applications: Fabrication, morphology, and electrical properties". *Frontiers in neuroengineering* 5 (2012), p. 8.

[9] Aviad Hai, Joseph Shappir, and Micha E Spira. "In-cell recordings by extracellular microelectrodes". *Nature methods* 7.3 (2010), p. 200.

[10] Aviad Hai, Joseph Shappir, and Micha E Spira. "Long-term, multisite, parallel, in-cell recording and stimulation by an array of extracellular microelectrodes". *Journal of neurophysiology* 104.1 (2010), pp. 559–568.

[11] Aviad Hai and Micha E Spira. "On-chip electroporation, membrane repair dynamics and transient in-cell recordings by arrays of gold mushroom-shaped microelectrodes". *Lab on a Chip* 12.16 (2012), pp. 2865–2873.

[12] Aviad Hai et al. "Spine-shaped gold protrusions improve the adherence and electrical coupling of neurons with the surface of micro-electronic devices". *Journal of The Royal Society Interface* 6.41 (2009), pp. 1153–1165.

[13] AL Hodgkin and AF Huxley. "A quantitative description of membrane current and its application to conduction and excitation in nerve". *Bulletin of mathematical biology* 52.1-2 (1990), pp. 25–71.

[14] Martin Jenkner and Peter Fromherz. "Bistability of membrane conductance in cell adhesion observed in a neuron transistor". *Physical review letters* 79.23 (1997), p. 4705.

[15] Ziliang Carter Lin et al. "Accurate nanoelectrode recording of human pluripotent stem cell-derived cardiomyocytes for assaying drugs and modeling disease". *Microsystems & Nanoengineering* 3 (2017), p. 16080.

[16] Paolo Massobrio, Giuseppe Massobrio, and Sergio Martinoia. "Interfacing cultured neurons to microtransducers arrays: a review of the neuro-electronic junction models". *Frontiers in neuroscience* 10 (2016), p. 282.

[17] Thomas Meyer et al. "Micro-electrode arrays in cardiac safety pharmacology". *Drug Safety* 27.11 (2004), pp. 763–772.

[18] Erwin Neher and Bert Sakmann. "The patch clamp technique". *Scientific American* 266.3 (1992), pp. 44–51.

[19] Walther Nernst. "Die elektromotorische wirksamkeit der jonen". *Zeitschrift für physikalische Chemie* 4.1 (1889), pp. 129–181.

[20] Marie Engelene J Obien et al. "Revealing neuronal function through microelectrode array recordings". *Frontiers in neuroscience* 8 (2015), p. 423.

[21] Silviya M Ojovan et al. "A feasibility study of multi-site, intracellular recordings from mammalian neurons by extracellular gold mushroom-shaped microelectrodes". *Scientific reports* 5 (2015), p. 14100.

[22] AG Petrov, RL Ramsey, and PNR Usherwood. "Curvature-electric effects in artificial and natural membranes studied using patch-clamp techniques". *European Biophysics Journal* 17.1 (1989), pp. 13–17.

[23] David A Robinson. "The electrical properties of metal microelectrodes". *Proceedings of the IEEE* 56.6 (1968), pp. 1065–1071.

[24] Kwang Sun Ryu et al. "Poly (ethylenedioxythiophene)(PEDOT) as polymer electrode in redox supercapacitor". *Electrochimica acta* 50.2-3 (2004), pp. 843–847.

[25] Hideki Shirakawa et al. "Synthesis of electrically conducting organic polymers: halogen derivatives of polyacetylene,(CH) x". *Journal of the Chemical Society, Chemical Communications* 16 (1977), pp. 578–580.

[26] Nava Shmoel et al. "Multisite electrophysiological recordings by self-assembled loose-patch-like junctions between cultured hippocampal neurons and mushroom-shaped microelectrodes". *Scientific reports* 6 (2016), p. 27110.

[27] Micha E Spira and Aviad Hai. "Multi-electrode array technologies for neuroscience and cardiology". *Nature nanotechnology* 8.2 (2013), p. 83.

[28] Micha E Spira et al. "Improved neuronal adhesion to the surface of electronic device by engulfment of protruding micro-nails fabricated on the chip surface". *Solid-State Sensors, Actuators and Microsystems Conference, 2007. TRANSDUCERS 2007. International*. IEEE. 2007, pp. 1247–1250.

[29] Micha E Spira et al. "Multisite Attenuated Intracellular Recordings by Extracellular Multielectrode Arrays, a Perspective". *Frontiers in neuroscience* 12 (2018), p. 212.

[30] Alfred Stett et al. "Biological application of microelectrode arrays in drug discovery and basic research". *Analytical and bioanalytical chemistry* 377.3 (2003), pp. 486–495.

[31] "Textbook of Medical Physiology". Elsevier, 2006. Chap. 1.

[32] C. Thomas et al. "A miniature microelectrode array to monitor the bioelectric activity of cultured cells". *Experimental cell research* 74 (1972), pp. 61–66.

[33] S Trasatti and OA Petrii. "Real surface area measurements in electrochemistry". *Pure and applied chemistry* 63.5 (1991), pp. 711–734.

[34] Tian Y Tsong. "Electroporation of cell membranes". *Biophysical journal* 60.2 (1991), pp. 297–306.

[35] Hainan Wang and Laurent Pilon. "Accurate simulations of electric double layer capacitance of ultramicroelectrodes". *The Journal of Physical Chemistry C* 115.33 (2011), pp. 16711–16719.

[36] Chong Xie et al. "Intracellular recording of action potentials by nanopillar electroporation". *Nature nanotechnology* 7.3 (2012), p. 185.

[37] Hitoshi Yamato, Masaki Ohwa, and Wolfgang Wernet. "Stability of polypyrrole and poly (3, 4-ethylenedioxythiophene) for biosensor application". *Journal of Electroanalytical Chemistry* 397.1-2 (1995), pp. 163–170.

[38] Martin L Yarmush et al. "Electroporation-based technologies for medicine: principles, applications, and challenges". *Annual review of biomedical engineering* 16 (2014).

[39] Günther Zeck. "Investigation of the Functional Retinal Output Using Microelectrode Arrays". *Glaucoma*. Springer, 2018, pp. 81–88.

[40] Wenting Zhao et al. "Nanoscale manipulation of membrane curvature for probing endocytosis in live cells". *Nature nanotechnology* 12.8 (2017), p. 750.